

Tijdschrift van het Nederlands Radiogenootschap

DEEL 20 No. 5

SEPTEMBER 1955

Shore-based radio aids to navigation on centimetric wavelength

by J. M. F. A. van Dijk, N. Schimmel and E. Goldbohm *)

SUMMARY

The problem of shore-based radar as a navigational aid for shipping is discussed from the system engineering point of view. A short review of the work carried out in the Netherlands, Belgium and Western Germany is given.

Radio aids to navigation have become more effective as the practical application of very high frequencies and pulse techniques were introduced. New navigational aids were born and in the past decade the mariner has been provided with instruments he never dreamt of before.

Fog and bad visibility still remain dreadful enemies, but the penetration of fog achieved by the use of narrow beams of electromagnetic waves of appropriate wavelength and pulses of fractions of microseconds have given to the mariner the tools to avoid collisions at sea and to make landfall easier.

Although marine radar is now widely used, the situation in thick weather at estuaries and entrances to inland ports is still the same as before: a great number of ships is anchoring and only a few go-getters dare to steam up, relying on their marine radar. Multiple echos caused by nearby ships, interference from other marine radar sets, shadow areas in river-bends and side-lobe effects may however cause extra danger by misinterpretation of the radar information.

In waterways, full of bends and lined with buildings along the banks, the picture on the marine radar screen does not extend around the following bend. No marine radar has yet

*) Netherlands Radar Research Establishment, Noordwijk-The Netherlands.

been devised, similar to the machine-gun recently announced, which is claimed to be able to fire around corners. Here the use of shore-based radar installations can definitely bring a solution, providing that great care is given to the siting, the technical specifications and the operational procedure of such systems, in other words: to the system engineering.

The International Meeting on Radio Aids to Navigation (IMRAM-conference), held in London in 1946, made the first recommendations for the use of shore-based radar and radar beacons.

The formulation of these recommendations with regard to this special application of radar was remarkably to the point.

I would like to quote it briefly:

"The object of the facilities at present provided by port and harbour authorities is to afford a ship a safe and easy entrance or exit and a safe anchorage or berth under all conditions of weather. It is obvious that radar can supplement these facilities very valuably by providing virtually instantaneous information of movements in the port area."

If the location of a shore-based radarstation is chosen judiciously and full advantage is taken of all the refinements, offered by modern radar technique, it is possible to achieve a radar picture, which is so sharp and distinct that the results are infinitely superior to those obtained by a radar installation on board of a ship, proceeding in the same area.

The low countries at the deltas of Rhine, Maas and Scheldt with the major ports Amsterdam, Rotterdam and Antwerp which are connected with the North Sea by long inland waterways and where navigation is frequently menaced by fog and bad visibility, form an ideal practising ground for this new technique of shore-based navigational aids.

The members of the conference*) have already been provided with a report of Captain H. Tichelman on the first shore-based radarstation installed on the European continent at Ymuiden, which was put into operation in November 1951. Another report was given by the Netherlands Radar Research Establishment on the development of what well may be considered at present as the most extensive system of shore-based radarstations in the world: the system for the New-Waterway and

*) International Conference on Lighthouses and other aids to Navigation, Scheveningen 1955.

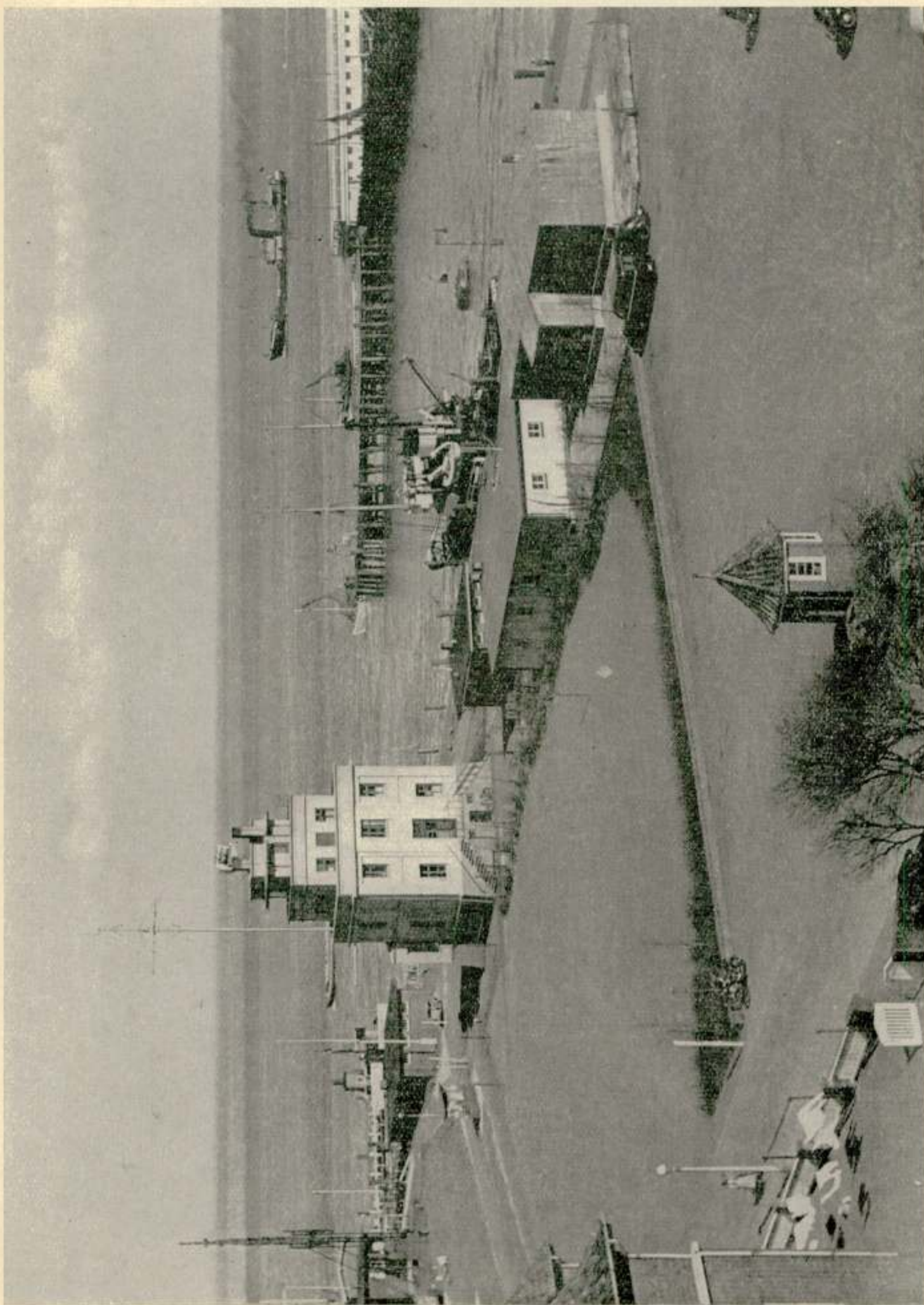


Fig. 1
Experimental shore based radar equipment is installed on the Semaphore at Cuxhaven for the Elbe estuary radar scheme



Fig. 2

Radar picture taken at Cuxhaven during Winter 1955
when the Elbe was covered with drift ice

the port of Rotterdam, which is now under construction and will be ready next year.

It is hoped that these two reports will supply to the conference sufficient technical and operational information on these systems. The picture however would not be complete if the conference were not informed on the further developments in this field.

It is now possible to give more information on recent experiments and survey work, carried out in connection with the siting of shore-based radarstations at the Scheldt estuary on Dutch and Belgian territory and in Western-Germany at the Elbe estuary.

These experiments and the survey work are being carried out by the Netherlands Radar Research Establishment on the request of the Belgian Ministry of Transport and the West-German Bundesverkehrsministerium.

The Netherlands Radar Research Establishment had placed at the disposal of the Bundesverkehrsministerium radar experts, trained personnel and experimental shore-based radar equipment. Two experimental shore-based radarstations have been

built under this scheme in Cuxhaven and in Brunsbüttelkoog and have been in operation with good results for more than a year under all conditions of weather, including a period in which the Elbe was partly covered by ice, which swept the navigational buoys away. During this experimental period the two stations have proved to be a most useful aid to navigation. Numerous reports of German pilots, who — equipped with portable V.H.F. transceivers — were taking an active part in these trials, have been a most valuable contribution to draw up recommendations for the operational procedure of the final system.

The Netherlands Radar Research Establishment has recently completed its studies on the Elbe-river radar scheme and has now submitted to the West-German Minister of Transport the final plans for a shore-based radar system which will cover the whole of the Elbe estuary from the Lightvessel ELBE I to Brunsbüttelkoog at the entrance of the Nord-Ostsee Kanal (Kiel canal).

In this plan it is recommended to build four shore-based radarstations with advanced technical specifications, each using 60 kW peak power magnetrons with variable frequency in the 3cm- or X-band. The horizontal beam of the radar antennae will have to be in the order of 0.6° , pulse-length 0.08 micro-second.

The method of presentation on the radar screen, which has a recommended diameter of 15", is of a special character. A pair of wandering electronic cursor lines will make it possible to provide to all ships under the coverage of the radar system accurate information in range and bearing relative to any desired position ashore or at sea within the range of the radarstation.

In the same way a number of wandering electronic lines can be switched in at will or will appear automatically on the screen to mark the navigational channel or any desired line of approach or leading-lines. This method of presentation is known as "Raplot".

At the Scheldt estuary a vast program is being carried out by the Netherlands Radar Research Establishment on the request of the Belgian Minister of Transport and with the full co-operation of the Netherlands authorities. A mobile survey is carried out along the shores of the Scheldt from Antwerp to the mouth of the river and on the coastline from Ostende to West-Kapelle.

The aim of this survey with mobile radar equipment is to allocate the proper sites for shore-based radarstations in this area and to determine their range and technical specifications.

After completion of the survey two experimental shore-based radarstations will be built at appropriate sites at the Scheldt estuary to gain operational experience with the latest technical developments in this field.

For those, who are in close touch with these problems, it will be obvious that the designer will not only have to adapt the system to the specific geographical situation of the area concerned, but that he must also base his design on the specific operational requirements of navigation in pilotage waters.

The system engineering of a shore-based radar system is a complex task of balancing out a great number of imponderables of a physical, nautical, geographical and economical character, thereby constantly keeping in mind the present state of development of the radar technique.

In most cases a survey with mobile radar equipment or at least a temporary installation of experimental radar equipment at suitable sites is essential. The mobile survey must be preceded by a careful study of the prevailing practice, the pilotage system, the topographical data and the local geographical situation.

The radar equipment for experimental use or mobile survey work in connection with shore-based radar system engineering must have a high degree of performance in range and bearing and must be provided with facilities to off-centre the picture and preferably have means to read accurately distance and bearing, not only from the centre of the screen, but also from any off-centre position to any desired position within the range of the equipment. Full facilities for taking photographs of the radar picture are needed. Observations of all seamarks and other points of importance to navigation should constantly be made and checked with the radar photographs to ensure that all the navigational marks, necessary to provide instantaneous navigational information, can be seen under all circumstances.

Means to erect the scanner quickly on 30 to 40 feet above ground level are indispensable; a power generating plant should be provided to ensure complete freedom of choice for the temporary sitings.

Armed with all these facilities, the mobile survey can start with the aim to allocate the proper sites of the minimum number of stations, necessary to give complete radar coverage in



Fig. 3

Shore based radar equipment on mobile survey for the Scheldt estuary radar scheme

the area concerned. The technical specifications of each of these stations are meanwhile being considered and gradually take a definite shape. It will be obvious that advanced technical specifications necessitate further research and development work to solve some specific problems.

The identification of ships, coming under the coverage of a shore-based radarstation, has hitherto not been solved in a satisfactory way. A new method is now being investigated, whereby unambiguous identification can be obtained with a minimum of equipment to be taken on board by the pilot. Transmission of the radar pictures to an operational headquarter does no more constitute a technical problem and

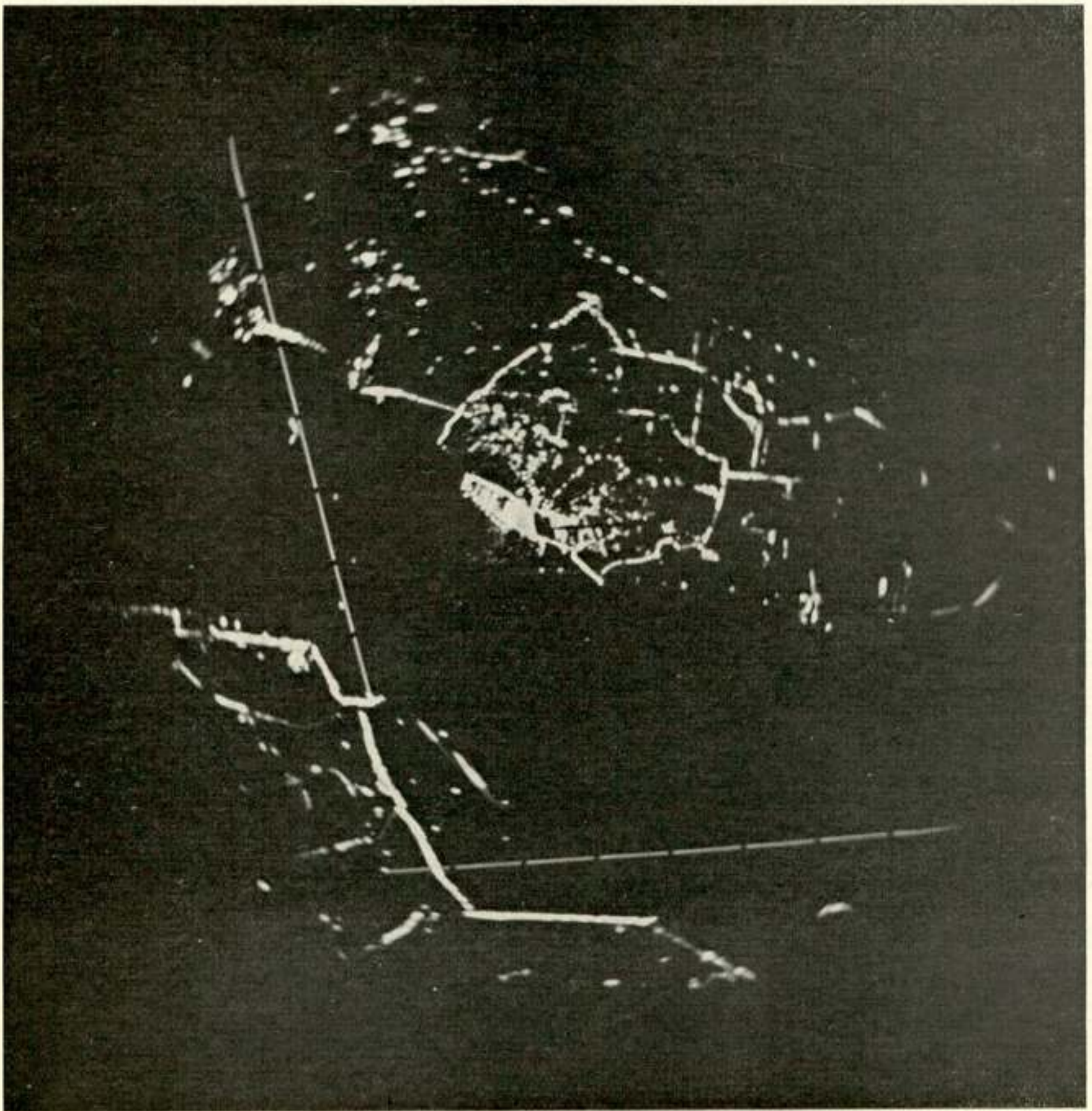


Fig. 4

Radar picture with two leading lines, taken at Waarde during the mobile survey for the Scheldt estuary radar scheme

may in some cases lead to a more elaborate and smooth-running system, which may help to economise the personnel problem. It remains questionable whether the transmission of radar pictures from shore to ship will pay itself and will be suitable for general adoption.

The use of circular polarisation may reduce undesired reflections from rain clouds.

A higher degree of definition may still be wanted for the last stage of berthing a ship in the inner port area and may well lead to the use of millimetric waves in the 8mm- or Q-band for these special circumstances.

In making landfall another group of radio aids to navigation, using microwaves, may well be suitable to support the landfall procedure and to improve the use of marine radar for navigation in coastal waters.

Lighthouses, lightvessels and lightbuoys, when transmitting electromagnetic waves in addition to the lightflashes, which are absorbed in thick weather, may help to identify these navigational marks in spite of fog.

In the Netherlands both Ramark and Racon are being developed for this purpose by the Netherlands Radar Research Establishment and a report on a newly developed Ramark installation will be given to the conference, followed by a demonstration on June the 7th.



A ramark beacon for use with marine radars

by J. M. F. A. van Dijk, N. Schimmel and E. Goldbohm *)

SUMMARY

In this paper a broad band high power 3 cm-ramark equipment is described with a range of max. 30 miles. Propagation difficulties have been largely overcome by a diversity system of transmitting aerials. Elimination of the ramark signal from the ship's P.P.I. is made possible by use of the F.T.C. circuit in the marine radar. The specifications of this ramark and results of trials are discussed.

1. *Introduction*

1.1. A vast amount of experience is gained by the users of marine radars as installed nowadays on board thousands of merchant ships. It is generally accepted that some auxiliary aid would be useful for the purpose of identification of insufficiently characteristic coastlines and of lightvessels. This navigational aid should be used during the last phase in making landfall and for coastal navigation, its useful range being from 3—30 miles off shore.

1.2. In view of this problem two types of experimental beacons have been produced, which are known as ramarks and racons, the former giving bearing information only, the latter range information as well. While the American radar-beacons are working in a special beacon band (9300—9320 Mc/s) outside the band allocated for marine radar, U.K. development was aiming at a beacon, covering the whole mercantile marine radarband, eliminating the need for the provision of a separate R.F. head, tuned to the beacon frequency, in the marine radar equipment.

2. *Existing radarbeacons*

2.1. Up till now radarbeacons have been established on an experimental basis only. The beaconband types can be used only in conjunction with radarequipment provided with specially built in R.F. heads for the band 9300—9320 Mc/s. It is clear that the application of this type of beacon is therefore limited and in view of the fact that many thousands of modern radars, installed on board of merchant ships, have not this facility and cannot even be modified in this respect, operational use of these types of beacons seems very remote.

*) Netherlands Radar Research Establishment, Noordwijk, The Netherlands.

2.2. The main development of radarband beacons was done up till recently in the U.K. A Racon type beacon was developed by A.S.R.E.¹⁾ after earlier work on a Ramark, operating in the marine radarband, and temporarily installed at St. Catherine's Lighthouse²⁾. It is outside the scope of this article to enlarge upon the Racon type of beacons. The British Ramark mentioned above used normal types of klystrons, six of which were needed for complete coverage of the marine radar band. The power output however was insufficient for reliable long range performance and a very annoying shortcoming of these beacons is the presence of zones of minimum signal caused by interference between the direct radiation and the one reflected by the surface of the sea³⁾.

From an earlier paper of D. G. Kiely and W. R. Carter⁴⁾ it was already known that very deep fading was measured in the propagation of 3-cm waves over a seapath during experiments carried out between July 1950 and January 1951 between Selsey Bill and Eastny Fort East, near Portsmouth harbour.

2.3. A study of the results of the work carried out in developing broadband ramark beacons shows clearly that mainly three factors were responsible for the fact that a generally acceptable solution for a ramark could not be reached. These factors were:

2.3.1. The non existence of an (electrically) tunable broad band oscillator with sufficient power output, of simple design and with a minimum of circuit requirements.

2.3.2. The existence of zones of minimum signal, making on-off coding ambiguous and confining the operational use seriously.

2.3.3. The almost complete masking of the radar picture at short ranges (see e.g. fig. 1 of ¹⁾).

1) "A Racon beacon for reception by Civil Marine Radars" by C. Randall-Cook (A.S.R.E.). Journal of the Institute of Navigation, Vol. VII, No. 2, April 1954.

2) A.S.R.E. Technical Note TX/49/7 1949. "Installation of Experimental Ramarks in Lighthouses" by N. Bell.

3) „The use of Radar at Sea". The Institute of Navigation, London, Hollis & Carter 1952, pp. 165 s.s. and fig. 140.

4) "An Experimental Study of fading in propagation at 3-cm wavelength over a sea path", D. G. Kiely, M.Sc., and W. A. Carter, B.Sc., Proceedings I.E.E., London, Vol. 99, Part III, No. 58, March 1952.

3. *Development in the Netherlands*

3.1. In 1953 the development of a high power broad band ramark was started by the Nederlandsch Radar Proefstation (Netherlands Radar Research Establishment) at Noordwijk. At that time a special tube became available, produced by Philips, Eindhoven, known as the multireflex klystron. This tube produces 10 Watts of continuous R.F. power at 3-cm and can be tuned over a band of 180 Mc/s at the rate of e.g. 50 times per second. Apart from this simultaneous modulation with frequencies of the order of kilocycles is possible.

Development was based upon the following considerations:

3.1.1. Zones of minimum or no signal should be eliminated.

3.1.2 Unambiguous on-off coding should be provided.

3.1.3. Reduction of the masking of the radar picture at short ranges should be pursued.

3.2. These considerations may be enlarged upon in the following paragraphs.

3.2.1. Elimination of zones of minimum signal. This effect is caused by the interference of the direct radiation and the one reflected by some plane e.g. the surface of the sea. Theoretically it is possible to eliminate this effect by using the principle of diversity transmission. For the purpose of testing out this system under operational conditions, a ramark transmitter (fig. 6), which will be described in some detail in 4.3, was temporarily installed in the semaphore at IJmuiden. The output could be switched by means of a waveguideswitch to one of two aerials of a broad band slotted waveguide type (see 4.2 and fig. 8) the lowest one being 54 ft above mean waterlevel, the highest one being 21 ft higher. The ramark signal was observed on a Decca Marine Radar type 12, installed on board the buoyage tender "Zaandam" which vessel was made available for the experiments through the co-operation of the Director of Pilotage of the district. During trials the effect of minimum signal zones could be observed and it was always possible to receive the ramark signal again by switching over to the other aerial.

A solution for operational use is the following. It is a good practice to duplicate shore based electronic navigational aids. This applies as well to ramarks; therefore in practice there will be two transmitters available anyway as part of the beacon equip-

ment. The best solution, and an economic one at the same time, will be to have two ramark transmitters, each connected with its own aerial and to choose the aerial heights such, that the wanted effect will be reached for varying heights of ships radar aerials as met in ships installations. In case of breakdown of one of the transmitters, there will still be a ramark signal, be it with the limitations of the presence of a minimum signal zone, which is always better than complete interruption of the service.

Although there has not yet been sufficient time available to investigate the effect of the diversity aerial system over longer periods in respect to the big fluctuations of signal strength over a sea path as experienced by single aerial systems (4) it is very probable that this problem is solved at the same time, reducing the wanted R.F. power to something of the order of 10 Watts.

3.2.2. Because of the elimination of minimum signal zones, on-off coding becomes a practical proposition.

Our belief is, that comparatively long off-periods, divided by short on-periods will be adequate for fulfilling the task of a ramark, e.g. 50 seconds off (or even longer) and 10 seconds on. In this case on the average the ramark signal will be depicted two to three times consecutively during each period of 1 minute which is sufficient to take a bearing.

This type of coding is to be preferred above the one using various H.F. modulation frequencies, because the shape of the signal (dots or dashes) depends to a high extent on the range scale used on the marine radar.

Apart from the possibility to overcome masking of the radar picture at short ranges by application of a suitable H.F. modulation frequency in conjunction with the F.T.C.-circuit of a marine radar, an on-off coding as outlined above leaves the radar picture under the worst circumstances unaffected during at least 80% of the time.

3.2.3. The provision of F.T.C. circuits in marine radars which can be switched on to overcome the effect of serious rainclutter has become more and more a standard feature of modern ship's radars. It may be stated that the modification to provide existing radars which have not this feature incorporated with such an anti-rain clutter device is only a minor one. An inves-

tigation into the time constants of F.T.C. circuits in present day ship's radars has shown that they differ rather widely. Theoretical considerations followed up by some experiments have shown that an H.F. modulation of 5–10 kc/s seems a good compromise to ensure the elimination of the ramark signal from the PPI picture by switching on the F.T.C.-circuit.

In the prototype equipment, described in some detail in 4.3, a wide range of modulating frequencies is available. The siting of a ramark is very important in view of the eventual masking of ship's radar pictures. We are of the opinion that the main purpose of a ramark is the provision of means to the user of marine radar to identify insufficiently characteristic targets along a coastline to promote the possibility of establishing his position with the aid of his radar. In this respect the beacon can be situated on such a site that shipping will never come closer than say 3 miles from the beacon, eliminating in this way the masking and cluttering up of the picture through side-lobe effects to a great extent. We are aware of the fact that this policy could not always be followed but in the majority of cases advantage could be taken of this method for a great deal. In case of ramarks installed on lightvessels the situation is different, ships passing them generally rather close. Apart from the possibility of using the F.T.C. circuit an intelligently chosen on-off coding might prove sufficient under these circumstances.

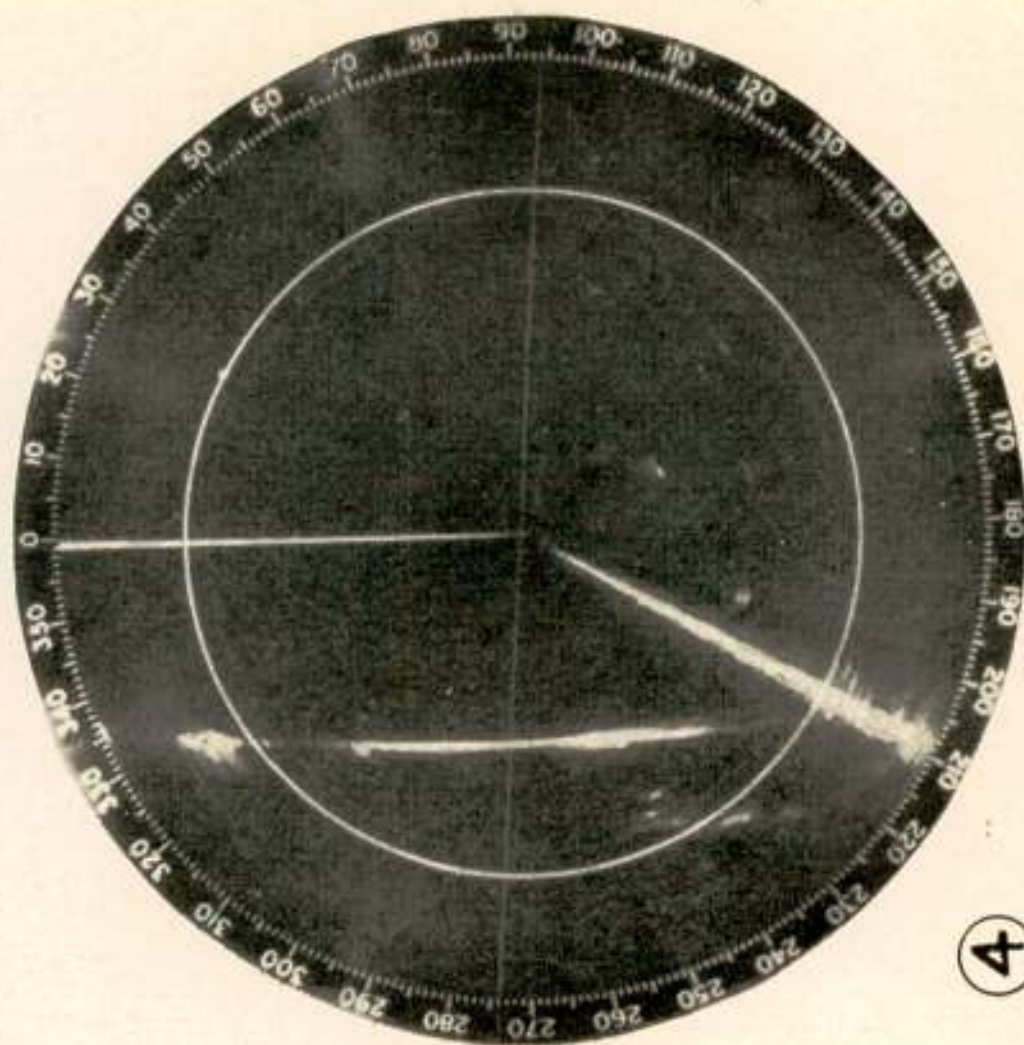
3.3. Based upon these considerations an experimental ramark was built (fig. 6) and was used during some sea-trials with the buoyage tender "Zaandam" mentioned above. At the time the photographs, which are reproduced in this report were taken, the lowest H.F. modulation was 75 kc/s, which was not sufficient to ensure complete elimination of the ramark signal, as shown on the photographs (fig. 2). It may be stated that the performance of a ramark beacon from the users' point of view is governed to a very great extent by the performance of the marine radar. The angular width of the ramark signal is entirely dependent on the radiation pattern of the radar aerial, its sidelobe level being of paramount importance at shorter ranges. It should be remembered that the sidelobes on the ramark signal as depicted on the P.P.I. have only half the attenuation expressed in db with respect to the main beam in comparison with the sidelobes visible of radartargets.

Apart from the marine radar as such, the siting on board

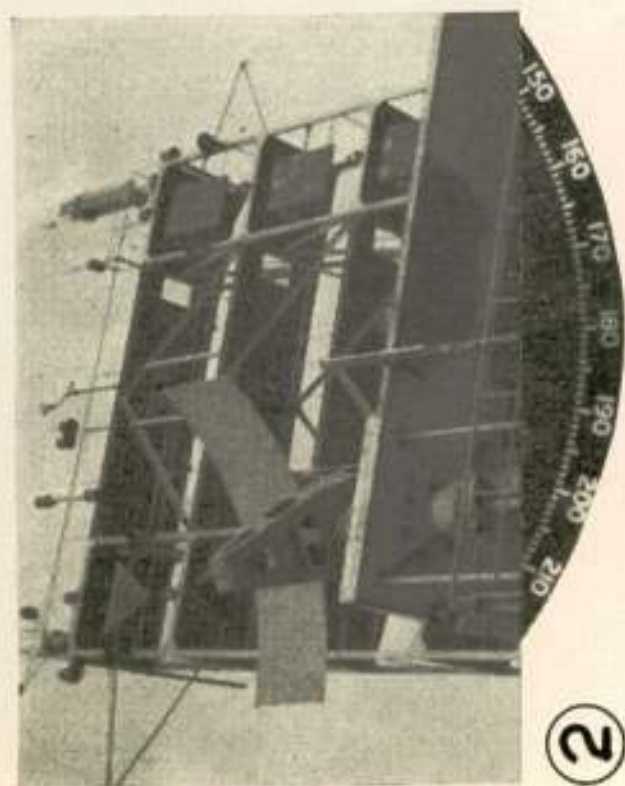
- Fig. 1. Range Scale P.P.I.: 3 N.M.
Beacon Range: 2.3 N.M.
Beacon modulation frequency: 75 kc/s
without Fast Time Constant. Bad sidelobes visible over 270°.
- Fig. 2. Range Scale P.P.I.: 3 N.M.
Beacon Range : 2.1 N.M.
Beacon modulation frequency: 75 kc/s
With F.T.C. Beacon signal considerably reduced.
Picture unfortunately disturbed by yawing of ship.
- Fig. 3. Range Scale P.P.I.; 25 N.M.
Beacon Range : 15 N.M.
Beacon modulation frequency: 300 kc/s.
Without F.T.C.
Bad yawing of the ship visible on ramark and 3 coastline echo signals.
- Fig. 4. Range Scale P.P.I.: 10 N.M.
Range Marker through beacon: 7,5 N.M.
Beacon modulation frequency: 75 kc/s.
Without F.T.C.
Picture disturbed by yawing.
- Fig. 5. Range Scale P.P.I.: 25 N.M.
Range Marker : 3 N.M.
Beacon Range : 21 N.M.
Beacon modulation frequency: 300 kc/s.
Without F.T.C. Yawing of ship.
- Fig. 6. Complete Ramark equipment in standard 19" rack as used during the experiments. Beacon aerial type slotted waveguide is also shown.
- Fig. 7. Close up of Philips multireflex klystron with magnet and waveguide.
- Fig. 8. Semaphore at IJmuiden.
Both beacon aeriels can be distinguished on the long vertical waveguiderun in the centre of the picture.



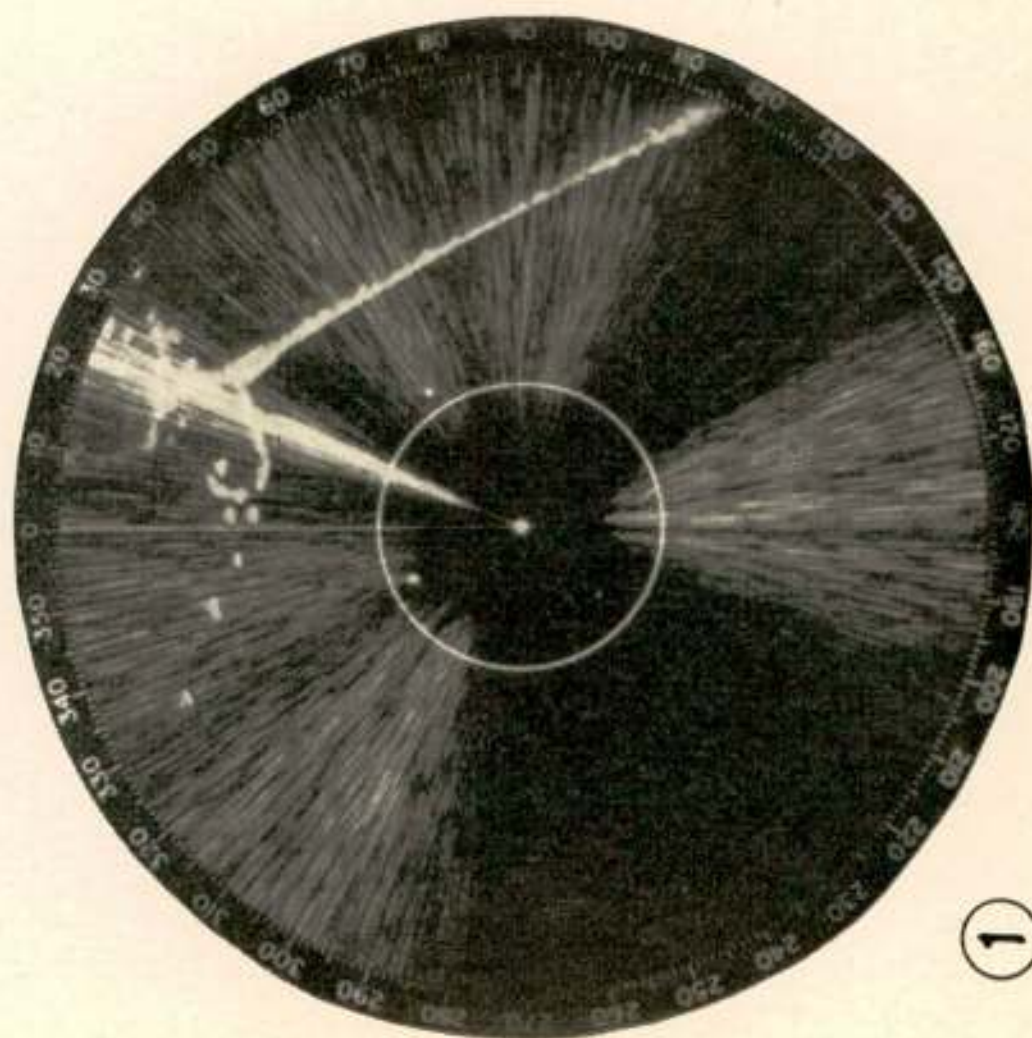
5



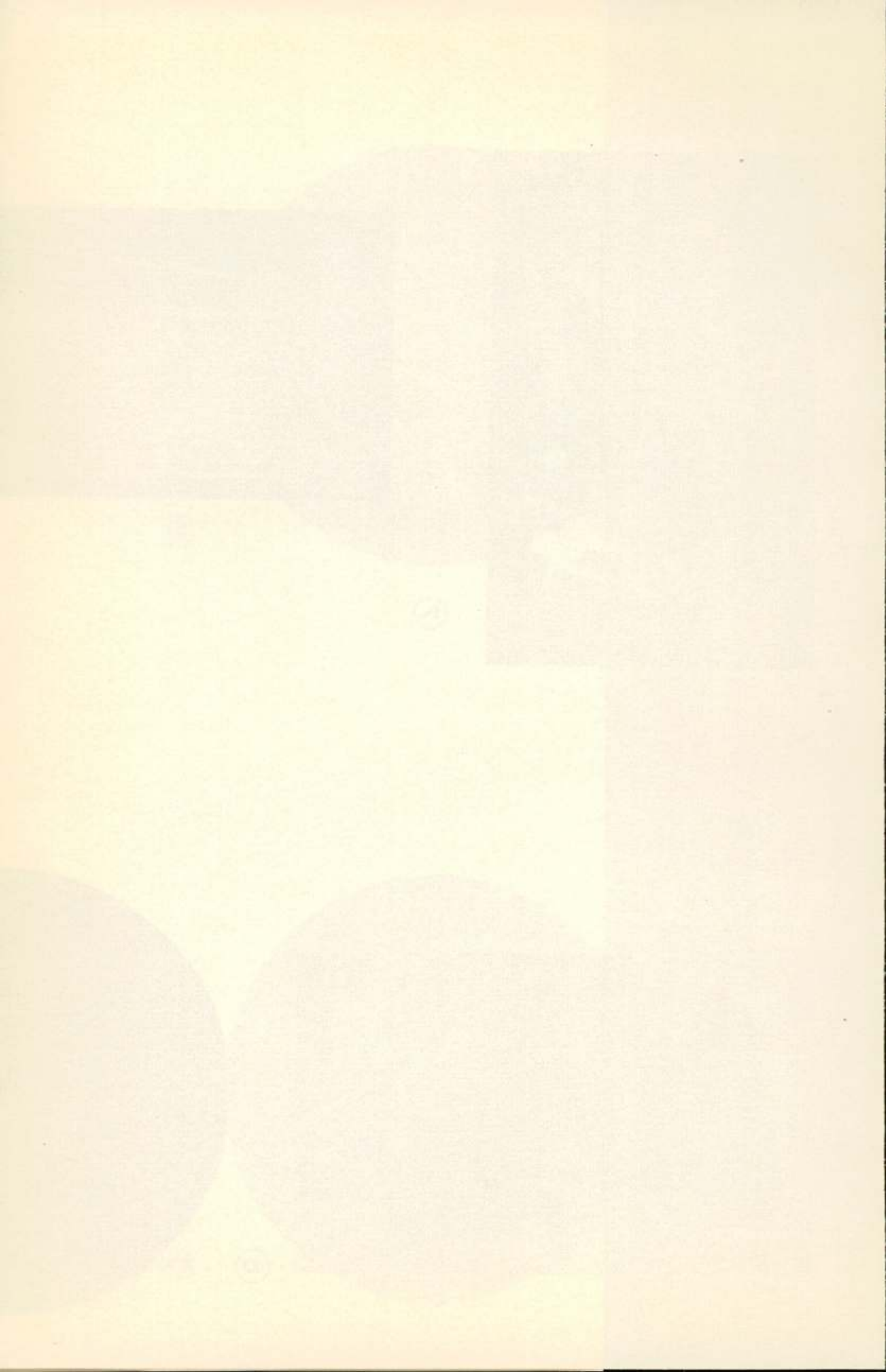
4



2



1



the ship is of great influence. The possibility to receive indirect radiation, reflected from parts of the ship's superstructure spoils the chance to receive a clean ramark signal and radaraerials installed close to a ship's mast or other steel structures may suffer seriously in sidelobe performance apart from the fact that unwanted large dead angles are present at the same time.

Unfortunately the aerial siting on board the buoyage tender "Zaandam" is in this respect far from ideal, although the special task this vessel has to fulfil, made another siting virtually impossible. The aerial was installed on a console in front of the very heavy bipod mast; at the time of writing this report it was tried to improve conditions by the installation of an oblique deflector plate between the aerial and this mast.

During trials ranges of 27 n.miles were achieved, which was beyond the radar horizon under the prevailing circumstances.

4. *Description of the ramark-equipment*

4.1. The ramark equipment consists of two main parts:

4.1.1. The aerial system.

4.1.2. The ramark transmitter.

Both parts will be described in some detail.

4.2. The aerial proper of the ramark consists of a broadband non resonant slotted waveguide, which radiates a narrow beam approx. normal to the array in the vertical plane and a wide beam (greater than 180°) in the horizontal plane giving coverage along e.g. a straight coastline. In order to obtain optimum gain of the aerial system, the length of the array has been determined consistent with such a width of the vertical beam, that the variation of signal strength on the horizon does not exceed approx. 3 db during a sweeping cycle of the oscillator. This variation originates from the fact, that the direction of max. radiation in the vertical plane varies with the frequency of the oscillator. This is a characteristic inherent to non resonant aerial arrays.

When the oscillator sweeps through the marine radar band, the vertical beam sweeps through 1,5 degrees.

The aerial mentioned above has been chosen to give a vertical beamwidth of 1,3 degrees.

Trials have shown, that the system has ample gain and that

indeed a reduction of the gain with a factor of 3 or 4 would leave an ample margin for operational use. In the case of lightvessels a wider vertical beam will be necessary anyway owing to the rolling of the ship.

Although this can be compensated by simple means (gimbals) a wider beam than 1,3 degrees seems advisable.

Also lightvessels will require an omnidirectional horizontal radiation pattern of the aerial. This can be achieved by a modification to the slotted waveguide system.

Concluding, the following specification may be suggested:

Horizontal pattern

Depends on local situation of Ramark. On straight or almost straight coastlines a 180° coverage is preferable. This is easily achieved with a single slotted waveguide. On lightvessels 360° patterns are required. Modification to the aerial will provide a solution.

Vertical pattern

Essentially only coverage of the horizon is necessary. Therefore narrow beam high gain aeriels are possible (in the vertical plane). However with regard to frequency sweep requirements and reduction of sidelobe interference on nearby ships (owing to sidelobes of the ships radar aerial) the gain and vertical beamwidth should be limited.

A compromise value is 4°–5°. On lightvessels a wider vertical beam (15–20°) is necessary or a simple stabilization of the aerial should be used (gimbals).

Polarization

Horizontal, since polarization for marine radar is horizontal.

Diversity

To reduce the interference effect as mentioned in 3.2.1 a diversity system of two aeriels has been tried in practice.

At the IJmuiden experiments the top aerial was at 75 ft above mean sea level, the bottom one at 54 ft. Both aeriels radiate incoherent frequencies, which can be used to advantage to increase mark space efficiency.

4.3. The ramark transmitter (fig. 6). The nucleus of the transmitter is the Philips multireflex klystron, which is shown with

its associated magnet in fig. 7. This klystron of all glass construction produces 10 Watts of continuous wave R.F. power with operating voltages of $2\frac{1}{2}$ to 3 kV. The efficiency is rather high and amounts to approx. 20%. The resonator of this klystron consists of a Lecher system incorporating a conducting ribbon, perpendicular to the magnetic field. The oscillating frequency of the klystron is determined by the Lecher system and the position of the ribbon. When an alternating current, e.g. 50 cycles AC is fed through this ribbon, this element starts to vibrate in the magnetic field resulting in a fast frequency sweep of 180 Mc/s, the klystron covering by these means the complete marine radar band.

The complete equipment is housed in a standard 19 inch rack and cabinet, which is about 4 feet high. In the top part of the cabinet the oscillator unit is housed. A frequency meter and a power output monitor are built in. The second chassis from the top contains the modulating circuits and a monitoring oscilloscope for checking the modulation and the performance of the klystron over the frequency band. The available modulation frequencies are 30—120 c/s for the low frequency part and 5, 10, 20, 40, 80 and 160 kc/s for the high frequency part.

The next chassis contains the necessary switching gear, fuses and other protective means with associated pilot lamps.

The fourth one houses the voltage stabilisation circuits, regulating the supply voltages for the multireflex klystron.

The power units are located in the bottom part of the cabinet.

In this experimental equipment a large number of built in meters are provided for checking all important currents and voltages.

The total power consumption is 400 Watts.

5. *Conclusions*

The following conclusions have been obtained during investigations with the abovementioned equipment.

It is estimated that 10 Watts of R.F. power is sufficient for operational use under all conditions. During the trials sufficient evidence has been collected that a diversity aerial system provides the possibility to cancel the effects of minimum signal zones. The judicious siting of the ramark beacon e.g. 3 miles from navigable channels will substantially reduce the masking effect

on a ship's P.P.I. In case this policy cannot be followed for obvious reasons, the F.T.C. circuit in marine radar in conjunction with a ramark beacon of appropriate H.F. characteristics can be used to advantage.

It is known that under certain circumstances distance information is desirable. A beacon providing this facility opens the possibility to eliminate all beacon signals on the P.P.I. between the ship and the beacon's position.

The solutions, known so far all suffer from saturation of the beacon and complexity of the equipment either on shore or shipborne.

Based upon the results hitherto reached with the new type of ramark, which does not exclude the application of the responder principle, further development work is in progress which may lead, as an alternative solution, to a new type of beacon, giving range information as well, at the same time taking full advantage of the features of the ramark as outlined in this publication.

The "Scenioscope", a new television camera tube

by P. Schagen *)

SUMMARY

Further investigations on the image iconoscope type of television camera tubes have led to the development of a new camera tube, the "Scenioscope". The target in this tube consists of semi-conductive glass, which makes the supply of negative charge possible from the signal plate through the target material to the surface of the target. The influence of the resistivity of the glass and of the thickness of the target sheet on the performance of the tube is considered.

The sensitivity of the "Scenioscope", which is at least five times as high as that of the image iconoscope, is also partly due to a considerably higher secondary-emission coefficient of the target coating.

Perfect picture quality with a very low noise level can be produced with an incident illumination of a few hundred lux ($f/D = 2$), whereas recognizable though noisy pictures without appreciable spurious signals have been made with light levels as low as 15 lux.

Introduction

A few years ago some papers on television camera tubes were read at a meeting of the "Nederlands Radio Genootschap", which were subsequently published in this journal (1).

From a comparison of the various camera tubes, presented in these papers, it appeared that the image iconoscope could produce excellent pictures, provided that the illumination level was not much below about 1000 to 1500 lux.

Although this light level is not difficult to establish in television studios, the artists may find the comparatively high temperature, due to the generation of heat by the lamps, somewhat troublesome. In theatres etc., where the normal illumination of the stage is insufficient for this purpose, the installation of extra lighting for a television broadcast is a rather expensive and sometimes also a difficult procedure.

The only television camera tube capable of producing acceptable picture quality at an incident illumination level of a few

*) Philips Research Laboratories, N.V. Philips' Gloeilampenfabrieken Eindhoven-Netherlands

hundred lux appeared to be the image orthicon. Apart from its higher sensitivity, however, this tube shows some distinct disadvantages compared with the image iconoscope.

For this reason further investigations were made in several research laboratories in Europe, with the aim of increasing the sensitivity of the image iconoscope, while at the same time maintaining its excellent picture quality.

In the Philips' Research Laboratories at Eindhoven, these investigations have resulted in the development of a new television camera tube, the "Scenioscope" (2). Although this tube shows a close resemblance to the image iconoscope type 5854 - its outward dimensions are exactly the same -, a fundamental difference in its mode of operation has yielded a gain in sensitivity of at least a factor 5 over the image iconoscope. Furthermore the ultimate limit to the use of the "Scenioscope" at

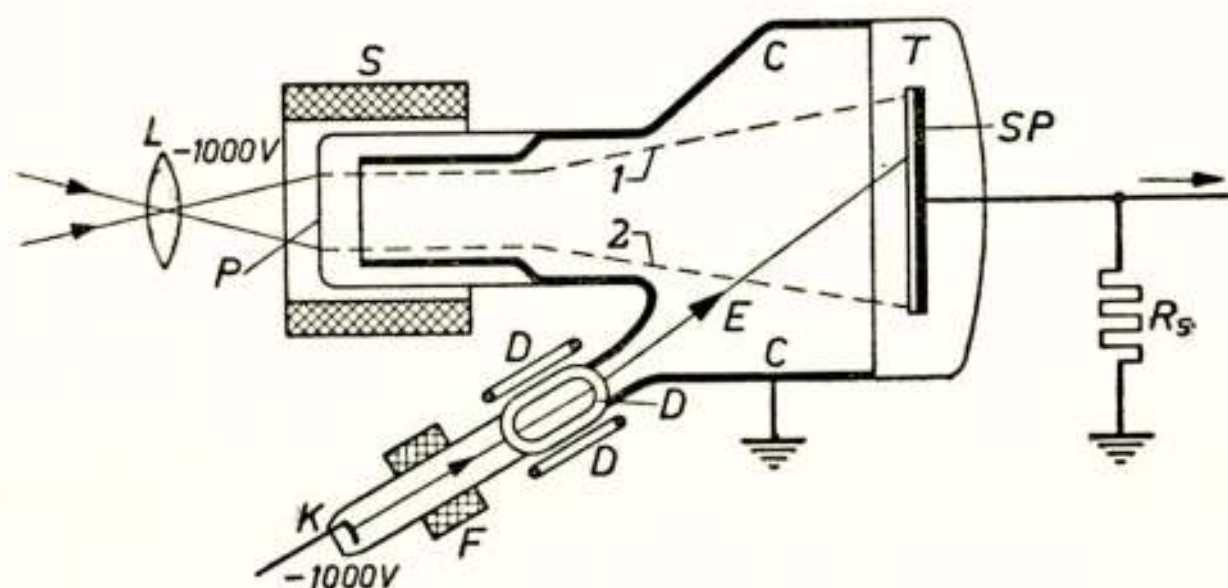


Fig. 1

Diagrammatic cross-section of the image iconoscope. *L* — lens; *P* — photo-cathode; *S* — coil of the magnetic electron lens; *T* — target (mica); *C* — collector; *E* — scanning beam supplied by an electron gun of which only the cathode, *K* — is shown in the diagram; *F* — focussing coil; *D* — deflecting coils; *SP* — signal plate; *R_s* signal resistor.

low light levels is set by the decreasing signal-to-noise ratio and no longer by the spurious signals, which appeared in the image-iconoscope pictures.

The "Scenioscope" produces excellent pictures, practically free of noise, at an incident illumination level of a few hundred lux, whereas during laboratory tests noisy though recognizable pictures have been made with light levels as low as 15 lux.

The image iconoscope

The mode of operation of the "Scenioscope" may be explained by first briefly recalling that of the image iconoscope.

In this tube (see figure 1) an optical image is projected on a semi-transparent photo-electric cathode. By means of a combined electric and magnetic lens every photo-electron, emitted under illumination by a certain picture element on the photo-cathode, is accelerated and directed to a corresponding element on the target.

The photo-electrons striking the target release more than one secondary electron each, thus forming a positive charge image on the target, which is scanned by an electron beam, stabilizing one target element after another a few volts above collector potential.

Part of the slow secondary electrons, released by fast photo-electrons or by the scanning beam, are captured by other target elements, where the potential may locally be even higher than collector potential. This "redistribution effect" is responsible for the gradual drop in potential of each target element between successive scans. As this potential becomes lower, the

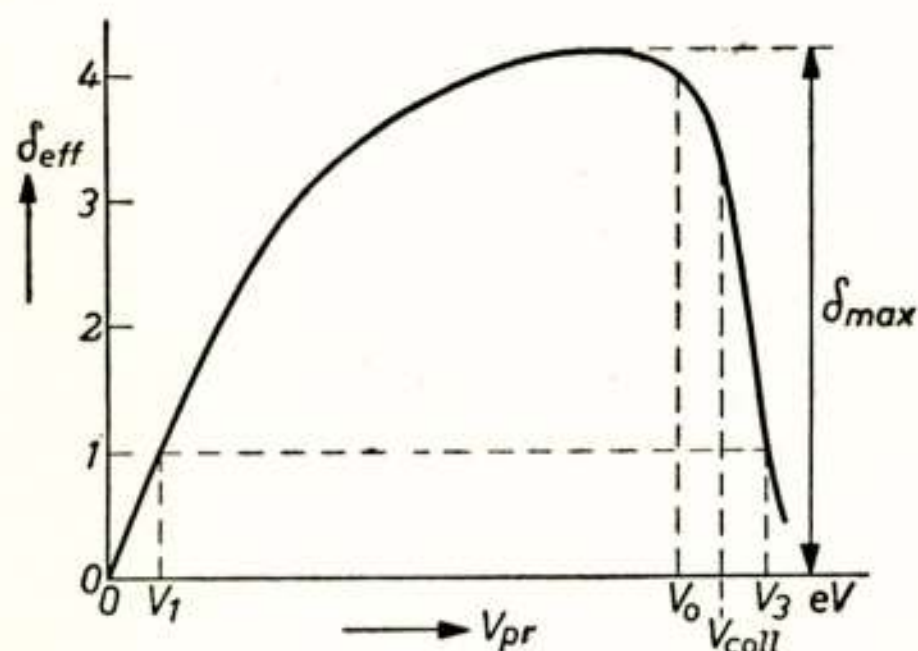


Fig 2

Effective secondary emission factor (δ_{eff}) of an insulator, plotted against the energy (V_{pr}) of the primary electrons.

$\delta_{eff} = 1$ when $V_{pr} = V_1$ or $V_{pr} = V_3$. Potential V_3 is one or two volts higher than the collector potential V_{coll} .

V_0 is the potential at which the flow of secondary electrons to the particular target element is completely cut off.

energy of an increasing part of the secondaries, released by the photo-electrons, is sufficiently high to let them escape to other target elements or to the collector. The effective secondary-emission coefficient, δ_{eff} , thus increases and so does the contribution of each photo-electron to the charge image.

Figure 2 shows schematically the relation between δ_{eff} and the potential of a target element, whereas figure 3 shows, also schematically, the potential variation of a target element between successive scans, with and without illumination.

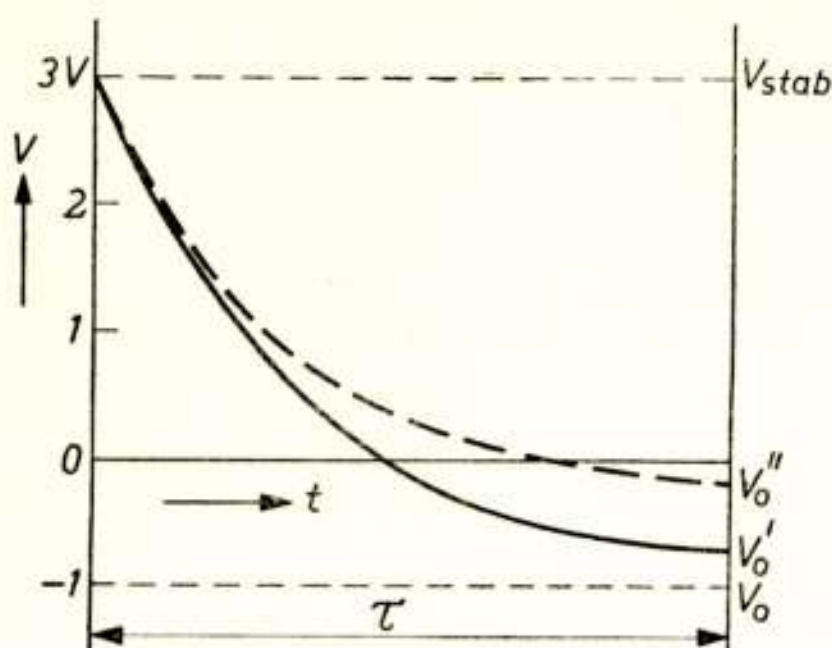


Fig. 3

Potential V of a target element in the image iconoscope, plotted against the time t , in the frame period between two scanings. Curve drawn as a solid line: photo-cathode not illuminated. Curve drawn as a dotted line: photo-cathode illuminated. Both curves start at the stabilizing potential V_{stab} (V_3 , see fig. 2) and approach V_0 asymptotically. By the end of interval τ , V drops to V'_0 or V''_0 . The contribution to the output signal is $V''_0 - V'_0$.

efficient of the photo-electrons increases only gradually from $\delta_{eff} \sim 1$ directly after each stabilization by the scanning beam. The illumination can therefore not be as effective as it would have been if the potential dropped more rapidly.

b. With increasing illumination the potential of the target elements falls even more slowly and these elements will, as a result, attract more redistribution electrons which partly neutralize the effect of the photo-electrons.

c. For different parts of the target the redistribution current to the target elements varies, resulting in the production of „spurious signals”, which do not correspond to the illumination. These spurious signals only decrease — both in absolute value and relative to the picture signal — with increasing illumination. The minimum light level, where the image iconoscope can still produce an acceptable picture, is therefore determined by the presence of these spurious signals and not by the decreasing signal-to-noise ratio.

Limitations to the sensitivity of the image iconoscope

The redistribution effect appears to be essential for the operation of the image iconoscope. Without the resulting drop in potential the target elements, once stabilized, would indefinitely retain their stabilization potential — with $\delta_{eff} = 1$ — under electron bombardment.

This effect, however, also sets the limit to the sensitivity of the image iconoscope for the following reasons:

a. Since the fall in potential of a target element is entirely determined by the limited number of slow electrons captured by this element, the effective secondary-emission co-

Possible methods of increasing the sensitivity

A method of increasing the sensitivity of the image iconoscope follows directly from the above considerations. If the potential of a target element can be made to fall more rapidly after stabilization, the effective secondary-emission coefficient, δ_{eff} , of the photo-electrons will reach its maximum value sooner and the photo-electrons can, as a result, contribute more to the formation of the charge image.

Increasing the beam current

A possible way of obtaining this effect seems to be given by increasing the redistribution current. This may be achieved by increasing the current of the scanning beam. The signal output of the tube does in fact rise with the beam current, but only to a limited extent, since the increased redistribution current is more attracted by the illuminated elements with their higher potentials. The signal-versus-beam current curve shows a maximum (3), whereas the spurious signals increase even more rapidly than the picture signal, making this method impractical. The drop in potential will therefore have to be achieved by means of a supply of negative charge to the target elements, which is independent of the scanning beam.

Showering the target with slow electrons

A more practical solution of this problem has been reached in the British "P.E.S.-photicon" (4) (Photo-Electrically-Stabilized) — the German "Riesel-Ikonoskop" (5).

In this tube the envelope surrounding the target has been provided with a semi-transparent photo-cathode, which is kept at collector potential and is illuminated by a circle of incandescent lamps. The resulting "drizzle" (hence the German name) of slow photo-electrons reaches the target, where a few auxiliary anodes, placed along the sides, direct most of these electrons to those parts of the target, where the redistribution current is too small.

The initial increase in sensitivity, caused by the more effective secondary emission of the photo-electrons, is partly counteracted, however, by the preference of the slow electrons for the illuminated target elements with their higher potentials. On

the other hand an important advantage over the normal image iconoscope is the nearly complete absence of spurious signals.

For this reason the P.E.S-photicon is claimed to need about half the illumination of the image iconoscope for good picture quality.

Supplying negative charge through the target

With the two above methods of forcing the potential of the target elements to fall more rapidly after each stabilization, negative charge is supplied by slow electrons reaching the elements from *outside* the target. Another possibility is the supply of negative charge *through* the target itself. The idea of employing a target with some — slight — conductivity was originally proposed both in England and in Germany, before the second world war, to increase the sensitivity of the iconoscope, and was first realised in an experimental tube, the „Halbleiter-Ikonoskop” (6).

Because this principle was not applied in the most advantageous manner, however, it never led to a practical tube.

In the Philips' Research Laboratories the principle of supplying negative charge through the target has been applied to the image iconoscope. This has resulted in the development of the “Scenioscope”, which will now be discussed in more detail.

The “Scenioscope”

Mode of operation

The fundamental difference between the “Scenioscope” and the image iconoscope is found in the target structure. The thin sheet of insulating mica in the image iconoscope has been replaced by a slightly thicker sheet of semi-conductive glass, which is backed with a conducting layer, the signal plate. A photograph of a mounted target is shown in figure 4.

The signal plate is given a lower potential than the collector anode, whereas the target elements are stabilized by the scanning beam at a few volts above collector potential. The resulting potential difference between the target elements at the surface and the signal plate at the back of the target sheet causes a current to flow through the target, which partly discharges the target elements between successive scans. The potential of these elements will, as a result, fall more rapidly after each stabilization. The target elements now only capture redistribution electrons while their potential is not more than a few volts

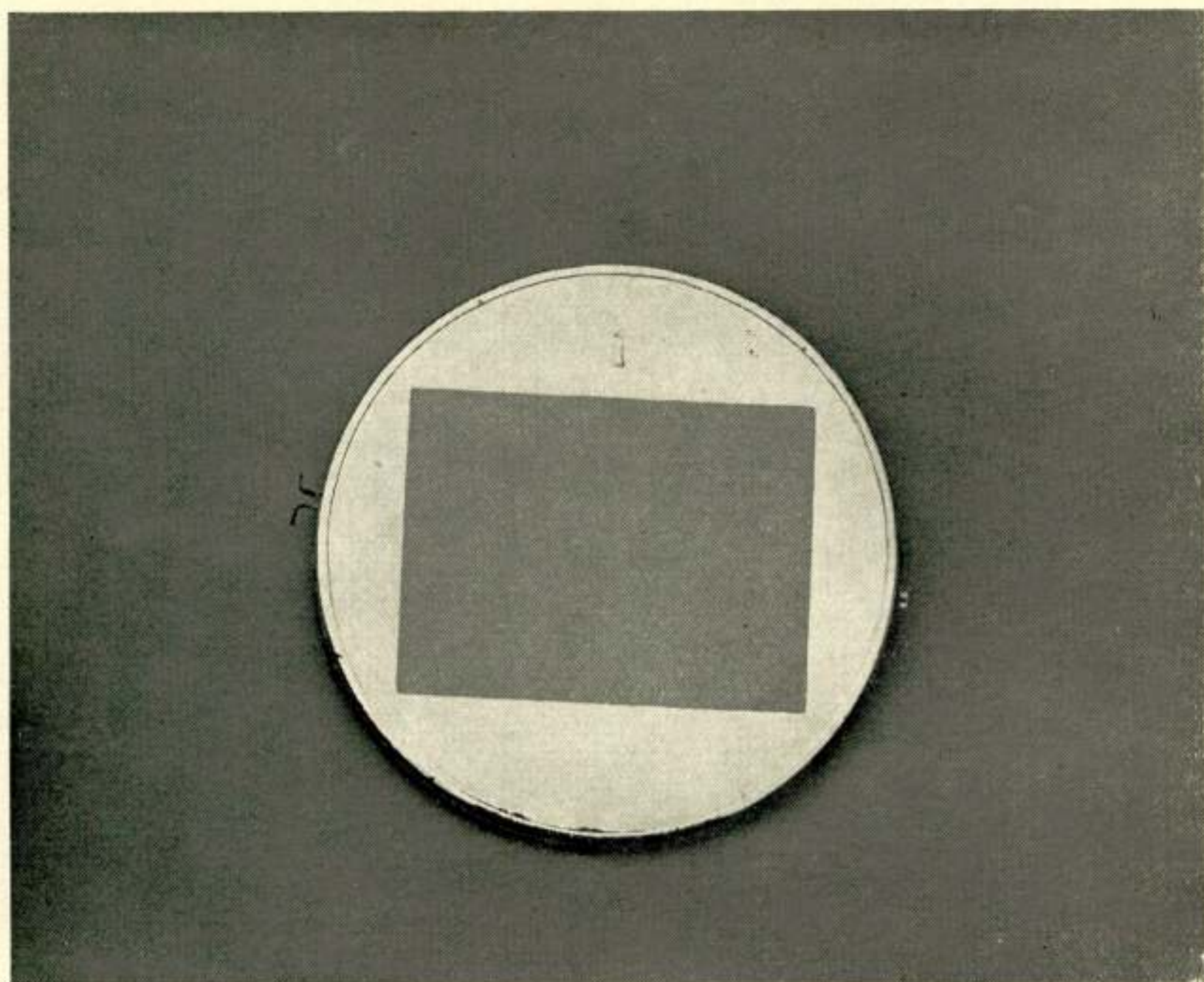


Fig. 4

The target of the „Scenioscope” is a “skin” of slightly conductive glass from 50 to 70 μ thick, on a metal ring. The size of the rectangular area scanned is 45 x 60 mm. The signal plate is a layer of metal on the back of the target.

below stabilization potential, whereas the discharging current through the target continues to flow throughout the time between two successive stabilizations, provided that the relaxation time R_0C_0 of the target material is sufficiently long compared with the frame period.

Since the current through the target is independent of the location of the element on the target, this current does not cause spurious signals. The redistribution current to an element should therefore be kept as small as possible, compared with the current through the target to avoid these spurious signals. This is a fundamental difference with the image iconoscope, where the redistribution effect is essential. In the “Scenioscope” it is only a secondary effect, which has to be avoided as much as possible.

The schematic diagram in figure 5 shows the potential of a

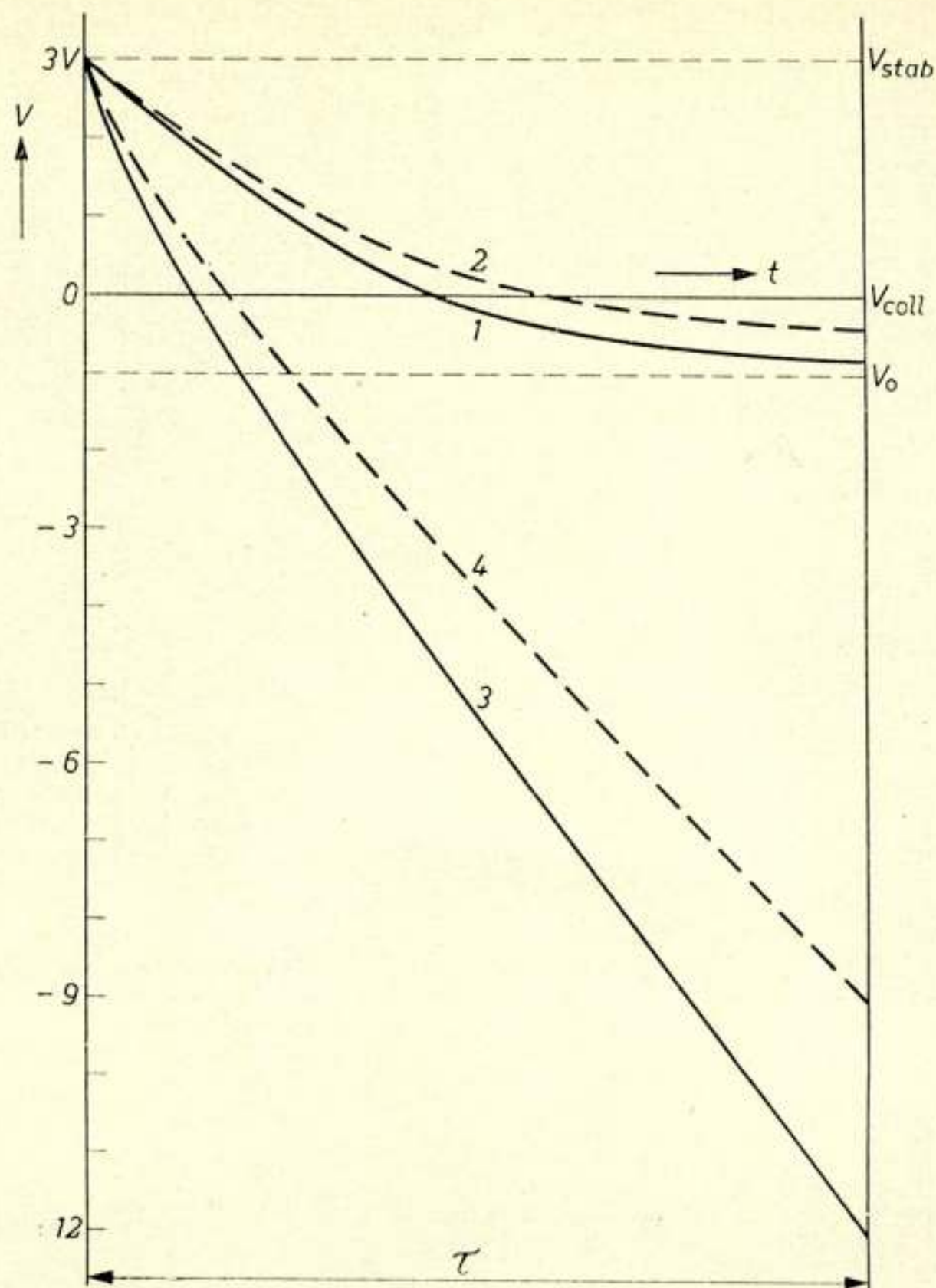


Fig. 5

1 and 2 are $V = f(t)$ curves, as shown in fig. 3, for the image iconoscope, 3 and 4 refer to the "Scenioscope", with slightly conductive target, signal plate potential negative, 3 for a non-illuminated, and 4 for a faintly illuminated photo-cathode.

target element, with and without illumination, between two successive scans. The corresponding curves for an image iconoscope have also been given again for comparison.

From the above considerations it follows that a rapid fall in potential of the target elements is desirable for two reasons:

a . The effective secondary-emission coefficient, δ_{eff} , of the photo-electrons will reach its maximum value sooner, thus increasing the sensitivity of the tube.

b. The redistribution current will be smaller and spurious signals will therefore be avoided.

There are two ways of increasing the speed at which the potential of the target elements drops: increasing the current through the target, and decreasing the capacitance of the target elements to the signal plate.

The permissible current through the target is limited by electrolysis of the glass, which cuts down the life of the tube. Furthermore local small differences in target thickness may cause spurious signals of a different nature, the amplitude of which is, of course, proportional to the current through the target.

A decrease in capacitance of the target elements to the signal plate — corresponding to an increase in target thickness — is limited by the requirements of good picture resolution and of a desirable gamma in the output characteristic, as will be shown later.

The resistivity and thickness of the target

Since the target material in the "Scenioscope" is not completely insulating, but semi-conducting, part of the positive charge built up by the photo-electrons on the various target elements will also be lost by conduction before the next scanning. The effect of this conduction on the charge image has been studied in a recent paper (7), the results of which will be summarized here.

The conductivity of the target material has two effects on the charge image. In the first place, image charge will leak *through* the target to the signal plate and will be lost before it can be removed by the scanning beam and contribute to the output signal of the tube. This results in a loss of sensitivity, which is determined by the relaxation time R_0C_0 of the target material, where R_0 is the resistance and C_0 the capacitance between the surface of the target and the signal plate, both per unit target area.

Figure 6 gives the relative signal output as a function of τ/R_0C_0 where τ denotes one frame period (0,04 sec in the European television systems).

If the loss of sensitivity may not be more than about 10%, figure 6 shows that the value of τ/R_0C_0 must not exceed 0,25. With a dielectric constant of the glass of 6 to 8, this condi-

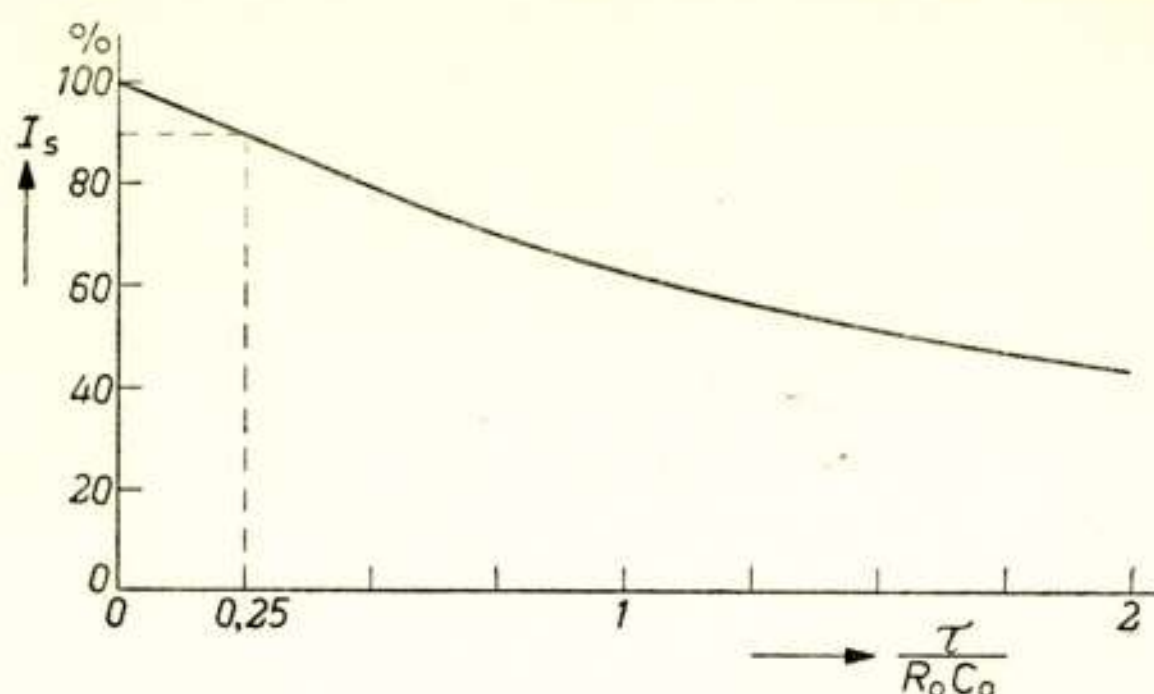


Fig. 6

Signal current (I_s : on relative scale), plotted as a function of τ/R_oC_o , for values of R_o and C_o consistent with an I_s equal to 90% of the maximum value ($\tau/R_oC_o = 0.25$).

tion requires a minimum specific resistivity ρ of the glass of $\rho = 3 \cdot 10^{11} \Omega\text{cm}$. On the other hand ρ should not be too high, since this might, for the same target current, introduce picture defects at the edges of target, which will be discussed later. The upper limit of ρ has therefore been chosen at about $\rho = 10^{12} \Omega\text{cm}$.*)

Secondly, positive charge will flow from target elements with more "illumination" to neighbouring elements with less "illumination", where the potential is lower. This is a conduction current *across* the target, resulting in a loss of picture resolution, which naturally affects the smallest picture details most. If, for instance, the picture were to consist of alternating strips with more and less "illumination" and a given contrast, this conduction across the target would decrease the depth of modulation in the charge image with decreasing width of the strips.

In order to study this effect more closely, a relative depth of modulation M may be defined as the ratio of the depth of modulation in the charge image just before the next scanning for a width D of the strips to that where half the target is

*) N.B. The specific resistivity of glass varies with the temperature. The values of ρ mentioned above apply to the working temperature of the tube, which should therefore be kept between certain limits. For the "Scenioscope" this temperature range has been chosen between 35° and 45° C. The corresponding values of ρ at room temperature are roughly between 10^{12} and $3 \cdot 10^{12} \Omega\text{cm}$.

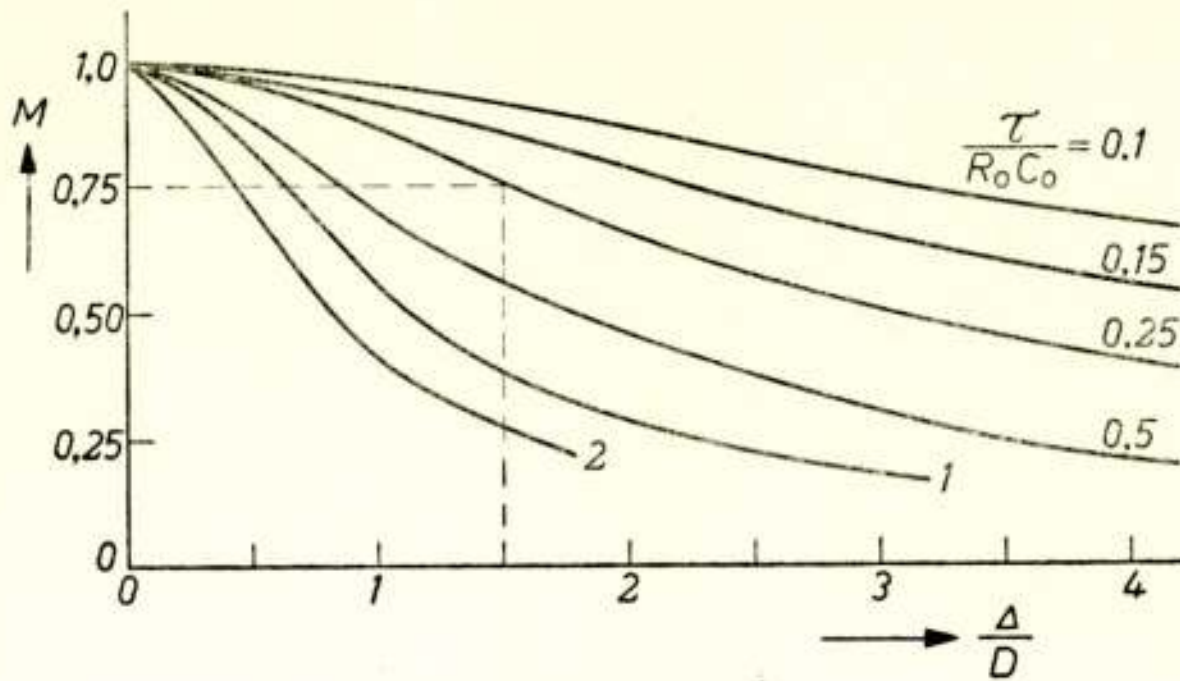


Fig. 7

Relative modulation depth M of the potential image on the target, plotted against Δ/D ($\Delta =$ thickness of target, D width of beams in a picture comprising black and white beams), with τ/R_0C_0 as parameter. For $\tau/R_0C_0 = 0.25$, Δ/D must not exceed roughly the value 1.

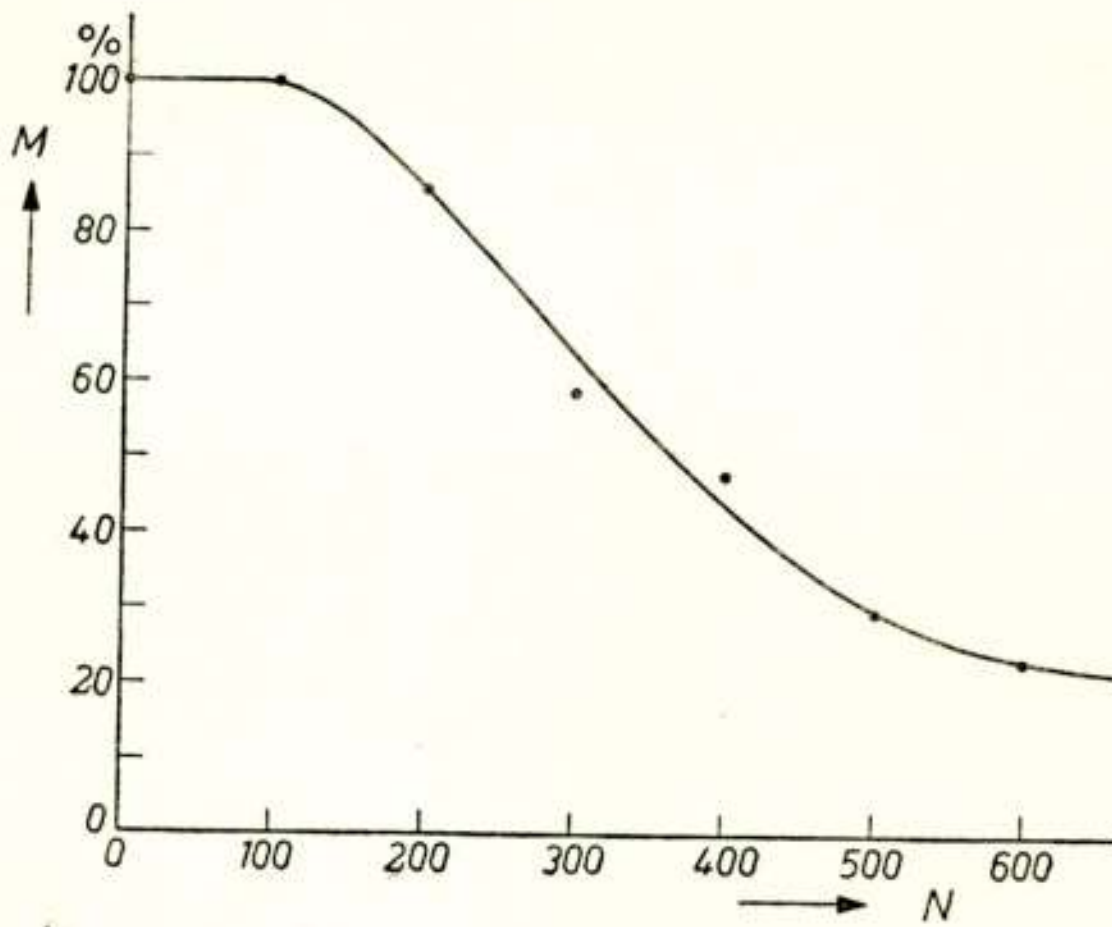


Fig. 8

Relative modulation depth M in the output signal of the "Scenioscope" in the centre of the picture, plotted against the number of lines per frame N .

"illuminated" and the other half is not. M may then be calculated for different values of τ/R_0C_0 as a function of Δ/D , where Δ represents the thickness of the target.

The results of this calculation are laid down in figure 7.

The diameter of the smallest details in the picture is equal

to the diameter of one picture element, corresponding to the width of one scanning line. For a television system with 625 lines, this diameter equals about 75μ on the target of the "Scenioscope". If the relative depth of modulation M in the finest details of the charge image on the target is not allowed to be more than 10% smaller than on an insulating target, figure 7 shows that with $\tau/R_o C_o = 0,25$, Δ/D should not exceed the value 1. The thickness of the target Δ should therefore not be more than about 75μ . In the "Scenioscope," Δ lies between 50 and 70μ and the picture resolution actually obtained differs very little from that obtained with the image iconoscope. Figure 8 shows the relative depth of modulation in the uncorrected output signal of the "Scenioscope" for the centre of the picture as a function of the line number.

The influence of the negative signal plate

The electric field above the surface of the target, which draws the secondary electrons to the collector, determines the stabilization potential of the various target elements. Without special precautions the field near the edges of the scanned target area might be considerably reduced by the influence of the negative signal plate. This would lead to a lower stabilization potential for these elements. The current through the target would be smaller and the scanning beam would accordingly deposit less positive charge during stabilization, similar to the effect of more illumination. In order to avoid bright edges showing in the reproduced picture, it appeared desirable to surround the scanned target area with a conducting frame, which can be given a potential slightly below that of the collector, thus effectively screening the negative signal plate. The adjustment of the scanning pattern on the target within this surrounding frame becomes more critical, however, with an increasing negative potential on the signal plate. For this reason the specific resistivity of the target material for a predetermined target current is limited, as was mentioned above.

The output characteristics of the "Scenioscope"

Once the resistivity of the target material and the thickness of the target have been chosen, the target current depends on the negative potential of the signal plate. This current de-

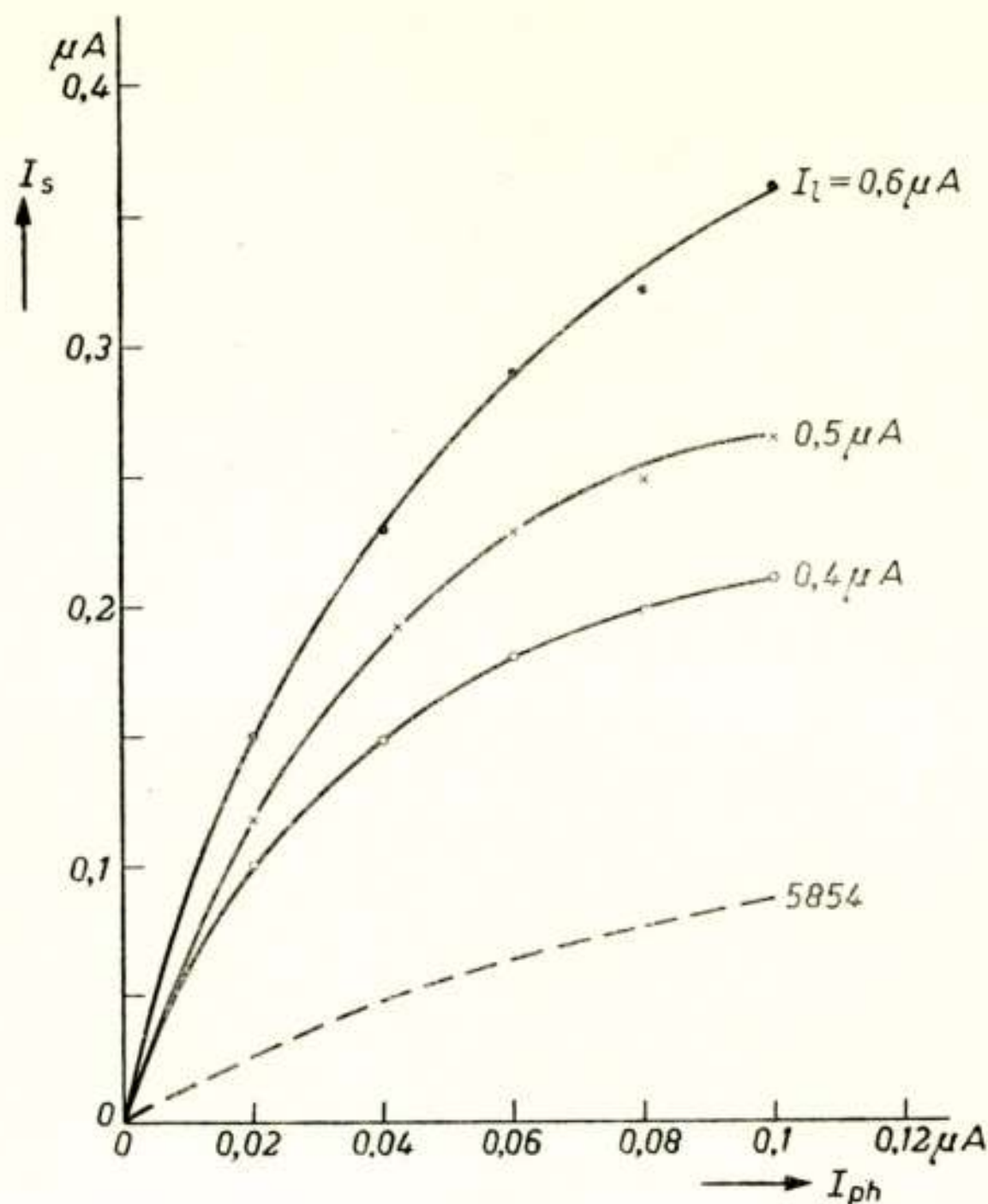


Fig. 9

Curve drawn as a solid line: I_s as a function of I_{ph} for the "Scenioscope", with the leakage current I_l through the glass target as a parameter (I_l measured in darkness). Curve drawn as a dotted line: $I_s = f(I_{ph})$ for image iconoscope 5854.

terminates the maximum output signal of the tube, because for the elements with the highest illumination the photo-current can, at most, replace the charge leaking away to the signal plate.

With a sufficiently high target current the potential of a target element with little illumination falls so rapidly that δ_{eff} reaches its maximum value δ_{max} shortly after each stabilization. The output characteristic of the tube, showing the signal current I_s as a function of the photo-current I_{ph} , is at first a straight line ($\gamma = 1$). With increasing illumination the drop in potential of a target element decreases and δ_{eff} of the photoelectrons reaches its maximum value later, while finally δ_{max} is not reached at all. As a result the output characteristic shows a gradual saturation, the shape of which is determined

by the capacitance of the target. For a smaller capacitance (thicker target) and equal target current, the saturation appears at higher photo-currents, and the characteristic will bend more sharply. With a greater capacitance the potential drop is smaller and the saturation sets in at lower photo-currents and is of a more gradual nature. This slightly reduces the sensitivity (less signal-current for equal photo-currents) but offers two advantages.

In the first place the gamma of the tube is now smaller than unity for a greater part of the output characteristic, similar to that in the image iconoscope, thus compensating for the gamma > 1 of the cathode-ray tube. The output signal needs no gamma-correction in this case.

The second advantage of the more gradual saturation in the output characteristic is gained by the fact that the maximum output signal now corresponds to much higher photo-currents, thus increasing the contrast range in the scene which the tube can still reproduce.

With the permissible target current of about $0.5 \mu\text{A}$ and the chosen target thickness of 50 to 70μ , the shape of the output characteristic appeared to be very favourable.

Some representative curves are given in figure 9 for three values of the target current. The typical output characteristic of the image iconoscope type 5854 has also been given for comparison.

Sensitivity

Whereas the increase in sensitivity of the "Scenioscope" over the image iconoscope is mainly due to the measures dealt with above, an important gain in sensitivity has also been achieved by the considerably higher secondary-emission coefficient of the target. It appeared possible to cover the surface of the glass target sheet with a very thin layer of material with a δ_{max} of 10 to 11, compared with the value of 4 to 5 in the image iconoscope, where the mica target sheet was coated with a thin layer of magnesium oxide.

The output characteristic of figure 9 shows that the sensitivity of the "Scenioscope" is not far below the maximum sensitivity which is theoretically possible with such a system: the ratio of I_s/I_{ph} at the lower end of the characteristic is about 7, whereas the theoretical value of I_s/I_{ph} for $\delta_{max} = 10$ equals about 11.

With decreasing illumination the picture quality deteriorates only by the decrease in signal-to-noise ratio and not by the spurious signals, as with the image iconoscope.

Perfect picture quality can be produced at an incident illumination level on the scene of a few hundred lux with a lens of $f/D = 2$. *)

In laboratory tests with some tubes this picture quality with a very low noise level could even be maintained below 100 lux, and recognizable though noisy pictures were made with light levels as low as 15 lux.

Apart from the difference in sensitivity, the "Scenioscope" and the image iconoscope will obviously have several features in common, since the photo-cathode, the electric and magnetic lens, and the electron gun providing the scanning beam are identical. The method of varying the field of view with electrical means (electric "zoom" lens (8)), discussed in the paper on the image iconoscope (1), can also be applied to the "Scenioscope".

References

- 1) H. Bruining, P. Schagen en J. C. Francken, Opneembuizen voor televisie. Tijdschr. Ned. Radio Gen. XVI-5, Sept. 1951.
- 2) P. Schagen, J. R. Boerman, J. H. J. Maartens en T. W. van Rijssel, De "Scenioscope", een nieuwe opneembuis voor televisie, Philips Tech. Tijdschr. 17, 173—182, Juni 1955.
- 3) P. Schagen, On the mechanism of high-velocity target stabilization and the mode of operation of television camera tubes of the image-iconoscope type, Philips Res. Rep. 6, 135—153, 1951.
- 4) J. E. Cope, L. W. Germany and R. Theile, Improvements in design and operation of image iconoscope type camera tubes, J. Brit. Inst. Rad. Engrs. 12, 139—149, 1952.
- 5) R. Theile, Die Signalerzeugung in Fernseh-Bildabtaströhren, Arch. elektr. Uebertragung 7, 15—27, 281—290 und 328—337, 1953.
- 6) G. Krawinkel, W. Kronjäger und H. Salo, Ueber einen speichernden Bildfänger mit halbleitendem Dielektrikum. Z. techn. Phys. 19, 63—73, 1938.
- 7) P. Schagen, Limiting resolution due to charge leakage in the scenioscope, a new television camera tube, Phil. Res. Rep. 10, 231—238, June 1955.
- 8) J. C. Francken and H. Bruining, Nieuwe ontwikkelingen aan de beeldiconoscoop, Phil. Tech. Tijdschr. 14, no 10, 282—290, Oct. 1952.

*) It has to be taken into account that the useful area of the photo-cathode in the "Scenioscope", as with the image iconoscope type 5854, has a diameter of 2 cm. The depth of focus in the pictures of the scenioscope with $f/D = 2$ is therefore comparable to that in the pictures of a tube with a diameter of the photo-cathode of 4 cm (like the image orthicon) with a lens aperture $f/D = 4$.

Electromagnetic Theory of Moving Matter II

by E. J. Post *)

SUMMARY

The present paper develops programme B of the previous paper and proceeds from the first order compatible Galilei kinematics and the "no aether" point of view.

The development benefits from a general distinction between physical quantities applying in general to phaenomenological theory. This distinction, which is based on the Neumann principle of crystal physics, suggests a definition of "state quantities" and "matter quantities". The discussion shows that state quantities appear only in the field equations and the transformation formulae of the state quantities. The equations of state on the other hand contain both quantities.

The application of these principles eases the way to the mathematical formulation given in the previous paper.

In the last sections, theory B is applied to some cases which cannot be solved by means of the usual classical formalism labelled as programme A in part I.

Introduction

As mentioned in the previous paper, the impossibility of establishing a velocity with respect to empty space is contained in the translational invariance of the empty space permeabilities ε_0 and μ_0 .

The other starting point, the Galilei kinematics, is contained in a general kinematical formula, which will be discussed at the beginning of the next section and appendix I.

The distinction and definition of state and matter quantities is covered by the following rules:

- I. A state quantity gives information about the state of a medium, independent of its properties.
- II. A matter quantity gives information about the properties of a medium, independent of its state.

The criterion for this distinction is indicated by the application of the Neumann principle. The matter quantity is subjected to the Neumann principle, the state quantity is not. The Neu-

*) Central Laboratories Netherlands P.T.T.

mann principle claims that any physical property of matter should be invariant for the group of symmetry operations determining the symmetry class of the substance in question. Electric and magnetic fields are state quantities in the sense of this distinction, relative permeabilities ε and μ are matter quantities. The latter are diagonal tensors with identical elements on the main diagonal for isotropic (and cubic) substances only (see appendix II- for applications of the Neumann principle).

Rule I implies the following rule about the transformation equations of state quantities.

III. The transformation equations of state quantities are independent of the nature of matter, otherwise they would contradict rule I.

A similar statement can be made about matter quantities.

IV. The transformation equations of matter quantities are independent of the state of matter, otherwise they would contradict rule II.

Rules III and IV are obvious and well known for a rotational change of coordinates, the direction cosines are the parameters of the transformation in this case. They are, however, equally true for a translational change of coordinates, the mutual velocity of the coordinate systems being the parameter of the transformation. The preceding considerations suggest the following classification of electromagnetic media, including empty space.

a. *Empty space*: The equations of state

$$\mathbf{D} = \varepsilon_0 \mathbf{E} \text{ and } \mathbf{B} = \mu_0 \mathbf{H} \quad (1)$$

are invariant for the group of rotations, improper rotations and translations of coordinate system.

b. *Isotropic matter*: The equations of state

$$\mathbf{D} = \varepsilon \varepsilon_0 \mathbf{E} \text{ and } \mathbf{B} = \mu \mu_0 \mathbf{H} \quad (2)$$

are defined with respect to a coordinate system fixed in the substance. They are invariant for the group of proper and improper rotations only.

c. *Anisotropic matter*: The equations of state

$$\mathbf{D} = \varepsilon \bar{\varepsilon} \mathbf{H} \text{ and } \mathbf{B} = \mu \bar{\mu} \mathbf{H} \quad (3)$$

are defined with respect to a coordinate system fixed in the

substance. They are invariant for the group of symmetry operations of the medium in question. The matter quantities $\bar{\epsilon}$ and $\bar{\mu}$ are tensors with, at most, six independent elements, if there is no symmetry. It will be clear from equations (1), (2) and (3) that the equations of state contain state quantities as well as matter quantities. The state quantities of a medium are required to satisfy the field equations.

It will appear in the next section that field equations contain state quantities only. This leads to the following rules:

- V. A field equation is independent of the nature of matter and independent of its motion.
- VI. An equation of state relates the state of matter to its properties, and henceforward contains both state quantities and matter quantities.

The features summarized in the six given rules are useful notions to keep in mind for an easy development of programme B. The physical parameters of empty space ϵ_0 and μ_0 are obviously not regarded as matter quantities.

Improper definition of state quantities as well as poor information about the equations of state may impair the formal distinction made in this section. The so called piezo-electric effect of some isotropic substances (Barium Titanate) f.i. is the product of the electrostrictive properties and the biasing field. It will be clear that this leads to matter quantities improperly defined in the sense of this section.

2. Transformation equations and field equations

Experimental observations are made on physical systems of finite size rather than on fields. The integral laws of Faraday-Maxwell, and Maxwell's extension (displacement current) of the law of Biot-Savart, are the result of observations on macro-physical systems. The mathematical analysis of these circuital laws invokes the concept of the time derivative of flux.

The flux ψ is related to a corresponding vectorfield \mathbf{A} by the surface integral:

$$\psi = \int_{\sigma} \mathbf{A} \cdot d\sigma \quad (4)$$

A change of ψ with time can be brought about by two independent sources i.e. the intrinsic change of the field \mathbf{A} with time and the change in position and shape of the surface σ

with time. The differentiation is expressed by the following well established mathematical formula, if the two sources operate simultaneously (see appendix I).

$$\frac{d\psi}{dt} = \frac{d}{dt} \int_{\sigma} \mathbf{A} \cdot d\boldsymbol{\sigma} = \int_{\sigma} \left\{ \frac{\partial \mathbf{A}}{\partial t} + \text{curl}(\mathbf{A} \times \mathbf{v}) + \mathbf{v} \text{div} \mathbf{A} \right\} \cdot d\boldsymbol{\sigma} \quad (5)$$

This theorem is based on the principles of Galilean kinematics. The first term in the integrant $\frac{\partial \mathbf{A}}{\partial t}$ corresponds to the intrinsic change with time of \mathbf{A} , the others are caused by the motion of the surface σ with the velocity \mathbf{v} . It is important to note that the integration and differentiation commute, only if the motion is uniform.

Equation (5) provides the essential mathematical tool to treat the circuital laws in their general form. They are:

$$\oint \mathbf{E}' \cdot d\xi = - \frac{d}{dt} \int_{\sigma} \mathbf{B} \cdot d\boldsymbol{\sigma} \quad \text{Faraday-Maxwell} \quad (6)$$

$$\oint \mathbf{H}' \cdot d\xi - \int_{\sigma} \mathbf{s}' \cdot d\boldsymbol{\sigma} = \frac{d}{dt} \int_{\sigma} \mathbf{D} \cdot d\boldsymbol{\sigma} \quad \text{Biot-Savart} \quad (7)$$

The line integrals in the left hand members with line element $d\xi$ are supposed to be the result of experimental observation. The contour of these integrals may be in motion with respect to the chosen coordinates. This suggests that the measurements are made in a frame of reference having a velocity with respect to the original coordinates. The symbols \mathbf{E}' and \mathbf{H}' are, therefore, provided with a dash to emphasize this distinction. The same holds for the current density \mathbf{s}' , as the current is defined as the amount of charge passing the aforementioned contour per unit of time.

The situation is different in the right hand members with the magnetic and electric inductions. It will be clear from the considerations in appendix I that the fields \mathbf{B} and \mathbf{D} are defined in the chosen coordinate system itself.

The application of Stokes' law and theorem (5) to the equations (6) and (7) gives:

$$\int_{\sigma} \text{curl}(\mathbf{E}' - \mathbf{v} \times \mathbf{B}) \cdot d\boldsymbol{\sigma} = - \int_{\sigma} \frac{\partial \mathbf{B}}{\partial t} \cdot d\boldsymbol{\sigma} \quad (8)$$

$$\int_{\sigma} \text{curl}(\mathbf{H}' + \mathbf{v} \times \mathbf{D}) \cdot d\boldsymbol{\sigma} = \int_{\sigma} \left\{ \frac{\partial \mathbf{D}}{\partial t} + \mathbf{s}' + \rho \mathbf{v} \right\} \cdot d\boldsymbol{\sigma}, \quad (9)$$

use being made of the fact that the divergence of the magnetic induction disappears, whereas the same operation on \mathbf{D} yields charge density ρ .*)

A stationary contour of the line integrals would have led to the equations:

$$\int_{\sigma} \text{curl } \mathbf{E} \cdot d\sigma = - \int_{\sigma} \frac{\partial}{\partial t} \mathbf{B} \cdot d\sigma \quad (10)$$

$$\int_{\sigma} \text{curl } \mathbf{H} \cdot d\sigma = \int_{\sigma} \frac{\partial}{\partial t} \mathbf{D} \cdot d\sigma + \int_{\sigma} \mathbf{s} \cdot d\sigma, \quad (11)$$

containing a set of coherent field quantities. Using the terminology of the previous section we may say; the state quantities \mathbf{E} , \mathbf{B} , \mathbf{D} , \mathbf{H} and \mathbf{s} are all defined with respect to the same frame of reference.

It is obvious that the following transformations are *sufficient* to reduce the equations (8) and (9) to (10) and (11):

$$\mathbf{E}' = \mathbf{E} + \mathbf{v} \times \mathbf{B} \quad (12)$$

$$\mathbf{H}' = \mathbf{H} - \mathbf{v} \times \mathbf{D} \quad (13)$$

$$\mathbf{s}' = \mathbf{s} - \rho \mathbf{v} \quad (14)$$

The corresponding field equations for a set of *coherent* state quantities are consequently:

$$\text{curl } \mathbf{E} = - \frac{\partial}{\partial t} \mathbf{B} \quad (15)$$

$$\text{curl } \mathbf{H} = \mathbf{s} + \frac{\partial \mathbf{D}}{\partial t} \quad (16)$$

The necessity of the formulae (12), (13) and (14) is suggested if we consider, that the transformations should form a group i.e. the result of two consecutive transformations again should have the form as given in (12), (13) and (14), the velocity parameter being the vectorial sum of the velocities of the two individual transformations. This together with the requirement of the existence of an identical transformation, restricts very considerably the possibilities for the addition of an arbitrary gradient field ($\text{curl grad} = 0$) in the formulae (12) and (13).

The analysis of the group properties of the equations (12), (13), moreover, informs us about the first-order nature of the transformation i.e. all terms of second-order and higher should

*) The divergence laws are not affected by a translation.

be discarded. This was to be expected, recalling the Galilean kinematics as one of the starting points of the theory.

The derivation of the transformations and field equations has been independent of the presence of matter, confirming the rules III and V of the previous section. Moreover, if the equations (12) and (13) are true in empty space, they still hold if we multiply them with the empty space permeabilities ϵ and μ . Use of the translational invariance of the latter leads to:

$$\mathbf{D}' = \mathbf{D} + \epsilon\mu\mathbf{v} \times \mathbf{H} \quad (17)$$

$$\mathbf{B}' = \mathbf{B} - \epsilon\mu\mathbf{v} \times \mathbf{E}, \quad (18)$$

application of rule III assures their independence of the presence of matter.

The first circuital law can be expressed in terms of a scalar and a vector potential, thus enabling the right hand member to be transformed into a line integral. Use of the corresponding theorem for the differentiation of a line integral (see appendix I formule VI) leads to a transformation of the scalar potential φ .

$$\varphi' = \varphi - \mathbf{v} \cdot \mathbf{A}, \quad (19)$$

\mathbf{A} being the vector potential. It is a peculiar feature that (19) like (14) is not subject to first-order restrictions to maintain its group properties.

The charge density ρ and the vector potential \mathbf{A} on the other hand have the property of being (Galilean) invariant for translations.

3. *The equations of state of non-conductive isotropic matter*

The equations of state of moving isotropic matter are easily derived using the transformation formulae (12, 13, 17, 18) and the equations (2) for stationary isotropic matter. If we take the reference system X' fixed in matter, the equations of state with respect to this system are

$$\mathbf{B}' = \mu\mu\mathbf{H}', \quad \mathbf{D}' = \epsilon\epsilon\mathbf{E}' \quad (2a)$$

Introducing a coordinate system X having a velocity $-\mathbf{u}$ with respect to X' fixed in the material medium yields:

$$\begin{aligned} (\mathbf{B} - \epsilon\mu\mathbf{u} \times \mathbf{E}) &= \mu\mu (\mathbf{H} - \mathbf{u} \times \mathbf{D}) \\ (\mathbf{D} + \epsilon\mu\mathbf{u} \times \mathbf{H}) &= \epsilon\epsilon (\mathbf{E} + \mathbf{u} \times \mathbf{B}). \end{aligned} \quad (20)$$

The equations (20) constitute the equations of state of a moving body. It is possible to transform (20) into an other first-order form which is more elucidating from a physical point of view. Rearrangement of the terms in (20) gives:

$$\begin{aligned}\mathbf{B} &= \mu\mu \mathbf{H} + \varepsilon\mu \mathbf{u} \times \mathbf{E} - \mu\mu \mathbf{u} \times \mathbf{D} \\ \mathbf{D} &= \varepsilon\varepsilon \mathbf{E} - \varepsilon\mu \mathbf{u} \times \mathbf{H} + \varepsilon\varepsilon \mathbf{u} \times \mathbf{B}.\end{aligned}\tag{21}$$

The equation (21) expresses the inductions \mathbf{B} and \mathbf{D} in the field strengths \mathbf{H} and \mathbf{E} except for the last first-order terms in the right hand member $-\mu\mu \mathbf{u} \times \mathbf{D}$ and $+\varepsilon\varepsilon \mathbf{u} \times \mathbf{B}$. Because of the first-order nature of (21) the \mathbf{D} and \mathbf{B} in the latter terms can be replaced by the zero-order approximations $\mathbf{B} = \mu\mu \mathbf{H}$ and $\mathbf{D} = \varepsilon\varepsilon \mathbf{E}$. The resulting equation, written in an appropriate "fourterminal" appearance, is the desired equation of state of moving isotropic matter.

$$\begin{aligned}\mathbf{D} &= \varepsilon\varepsilon \mathbf{E} - \varepsilon\varepsilon \mu\mu \left(1 - \frac{1}{\varepsilon\mu}\right) \mathbf{u} \times \mathbf{H} \\ \mathbf{B} &= + \varepsilon\varepsilon \mu\mu \left(1 - \frac{1}{\varepsilon\mu}\right) \mathbf{u} \times \mathbf{E} + \mu\mu \mathbf{H}\end{aligned}\tag{22}$$

For $\varepsilon = \mu = 1$, the equations (22) are reduced to the empty space equations of state (1), and as is to be expected, $\mathbf{u} = 0$ makes (2) the equations of isotropic stationary matter. It should be noted that Fresnel's convection coefficient $\left(1 - \frac{1}{\varepsilon\mu}\right)$, appears as a typical feature in the cross-coefficients of (22).

It is convenient to have the inverse set of equations:

$$\begin{aligned}\mathbf{E} &= \frac{1}{\varepsilon\varepsilon} \mathbf{D} + \left(1 - \frac{1}{\varepsilon\mu}\right) \mathbf{u} \times \mathbf{B} \\ \mathbf{H} &= - \left(1 - \frac{1}{\varepsilon\mu}\right) \mathbf{u} \times \mathbf{D} + \frac{1}{\mu\mu} \mathbf{B}\end{aligned}\tag{23}$$

The cross constants in (22) and (23) represent the "gyroscopic" properties of moving matter.

It is interesting to know that a fourterminal device based on the simultaneous application of the Röntgen and Wilson effects will constitute a non-reciprocal network. Tellegen (1) postulated the following relation between the state quantities of a hypothetical non-reciprocal stationary medium.

$$\begin{aligned} \mathbf{D} &= \varepsilon \mathbf{E} + \gamma \mathbf{H} \\ \mathbf{B} &= \gamma \mathbf{E} + \mu \mathbf{H} \end{aligned} \tag{24}$$

The feasibility of stationary matter having a $\gamma \neq 0$ deserves a discussion from the point of view of the second law of thermodynamics. An application of Neumann's principle shows that a "gyroscopic" effect (coefficient γ) cannot exist in stationary isotropic matter (see appendix II).

There are still other sets of equations of state with \mathbf{E} , \mathbf{B} and \mathbf{D} , \mathbf{H} , respectively as the dependent variables. This leads to the following equations:

$$\mathbf{E} = \frac{1}{\varepsilon \varepsilon_0} \mathbf{D} + \mu \mu_0 \left(1 - \frac{1}{\varepsilon \mu} \right) \mathbf{u} \times \mathbf{H} \tag{25}$$

$$\mathbf{B} = + \mu \mu_0 \left(1 - \frac{1}{\varepsilon \mu} \right) \mathbf{u} \times \mathbf{D} + \mu \mu_0 \mathbf{H}$$

$$\mathbf{D} = \varepsilon \varepsilon_0 \mathbf{E} - \varepsilon \varepsilon_0 \left(1 - \frac{1}{\varepsilon \mu} \right) \mathbf{u} \times \mathbf{B} \tag{26}$$

$$\mathbf{H} = - \varepsilon \varepsilon_0 \left(1 - \frac{1}{\varepsilon \mu} \right) \mathbf{u} \times \mathbf{E} + \frac{1}{\mu \mu_0} \mathbf{B}$$

This last choice of variables is more appropriate for the analysis of wave motion in moving matter.

4. *Wave propagation in moving non-conductive isotropic matter*

The general case of arbitrary directions of convection and wave propagation is somewhat cumbersome and involved. The essentials, however, may be studied for the one dimensional case.

The elimination of the successive state quantities between the Maxwell equations and the equations of state gives the following asymmetric wave equation:

$$\left\{ \frac{1}{\varepsilon \varepsilon_0 \mu \mu_0} \frac{\partial^2}{\partial x^2} - \frac{\partial^2}{\partial t^2} + 2v \left(1 - \frac{1}{\varepsilon \mu} \right) \frac{\partial}{\partial t} \frac{\partial}{\partial x} \right\} \psi = 0 \tag{27}$$

The function ψ stands for any of the state quantities. A wave solution

$$\psi = \psi_0 \exp i(\omega t - kx) \quad \begin{array}{l} \omega = \text{circular frequency} \\ k = \text{wave number} \end{array} \tag{28}$$

yields the frequency equation

$$\omega^2 = \frac{k^2}{\epsilon\epsilon_0\mu\mu_0} - 2v \left(1 - \frac{1}{\epsilon\mu} \right) \omega k. \quad (29)$$

Solving for the phase velocity $u' = \omega/k$ and remembering that first-order terms should be maintained only, leads indeed to the correct formula of drag

$$\frac{\omega}{k} = u' = u - v \left(1 - \frac{1}{\epsilon\mu} \right); \quad u = \sqrt{\frac{1}{\epsilon\epsilon_0\mu\mu_0}} \begin{cases} \text{phase velocity} \\ \text{in medium} \\ \text{at rest} \end{cases} \quad (30)$$

An experimental check of this formula for electric and magnetic permeable materials suggests an experiment in the range of cm wavelengths. Formula (30) cannot be derived on basis of a theory A (see part I).

5. *Miscellaneous applications*

The scope and significance of the transformation formulae are no doubt most readily appreciated if we analyse the mathematical and physical consequences for other field quantities, which can be derived from the fundamental set \mathbf{E} , \mathbf{B} , \mathbf{D} and \mathbf{H} .

Let us start with polarization \mathbf{P} and magnetization \mathbf{M} . A coherent definition of these quantities suggests that $(\mathbf{P}; \mathbf{D})$ and $(\mathbf{M}; \mathbf{H})$ have pairwise the same dimension. The following definitions satisfy this requirement:

$$\mathbf{P} \stackrel{def}{=} \mathbf{D} - \epsilon_0 \mathbf{E}; \quad \mathbf{M} \stackrel{def}{=} \frac{\mathbf{B}}{\mu_0} - \mathbf{H} \quad (31)$$

The definitions (31) together with the transformations lead to the following transformation rules for \mathbf{P} and \mathbf{M} :

$$\begin{aligned} \mathbf{P}' &= \mathbf{P} - \epsilon_0 \mathbf{v} \times \mathbf{M} \\ \mathbf{M}' &= \mathbf{M} + \mathbf{v} \times \mathbf{P} \end{aligned} \quad (32)$$

Using the equations (12, 13, 14, 17, 18, 19 and 32) the following scalars (or densities) can be found having the property of translational invariance:

$$\mathbf{E}' \cdot \mathbf{B}' = \mathbf{E} \cdot \mathbf{B} \quad (33)$$

$$\mathbf{D}' \cdot \mathbf{H}' = \mathbf{D} \cdot \mathbf{H} \quad (34)$$

$$\mathbf{P}' \cdot \mathbf{M}' = \mathbf{P} \cdot \mathbf{M} \quad (35)$$

$$\mathbf{E}' \cdot \mathbf{D}' - \mathbf{H}' \cdot \mathbf{B}' = \mathbf{E} \cdot \mathbf{D} - \mathbf{H} \cdot \mathbf{B} = L_I \quad (36)$$

$$\mathbf{E}' \cdot \mathbf{P}' + \mathbf{M}' \cdot \mathbf{B}' = \mathbf{E} \cdot \mathbf{P} + \mathbf{M} \cdot \mathbf{B} = L_{II} \quad (37)$$

$$\mathbf{s}' \cdot \mathbf{A}' - \rho' \varphi' = \mathbf{s} \cdot \mathbf{A} - \rho \varphi = L_{III}$$

It is a known, matter independent property, of electromagnetic wave motion that $\mathbf{E} \perp \mathbf{B}$ and $\mathbf{D} \perp \mathbf{H}$. Equations (33) and (34) claim this to be true (as a first-order effect) for moving matter as well. Similar considerations apply to (35).

The expression (36) is the Lagrangean of the electromagnetic field; it is due to its invariance that the Hamilton integral

$$\iint L_I d\tau dt \quad \begin{array}{l} dt = \text{time element} \\ d\tau = \text{space element} \end{array} \quad (38)$$

has an invariant meaning.

Equations (37) give the expressions for other Lagrangean densities L_{II} and L_{III} which are related to the forces exerted on matter. They disappear, identically, in empty space.

In a *linear* medium

$$E \stackrel{def}{=} \frac{1}{2} (\mathbf{E} \cdot \mathbf{D} + \mathbf{H} \cdot \mathbf{B}) \quad (39)$$

is an adequate and allowable definition of energy density and

$$\mathfrak{T} \stackrel{def}{=} -\frac{1}{2} (\mathbf{E} \cdot \mathbf{D} + \mathbf{H} \cdot \mathbf{B}) \mathbf{I} + \mathbf{E} \mathbf{D} + \mathbf{H} \mathbf{B} \quad (40)$$

defines Maxwell's tensor of "electro-magnetic stress" in matter. It should be noted that \mathfrak{T} is not necessarily symmetric if $(\mathbf{E}; \mathbf{D})$ or $(\mathbf{H}; \mathbf{B})$ have different directions (anisotropy).

Energy transport \mathbf{S} and momentum \mathbf{G} are defined by the usual equations:

$$\mathbf{S} \stackrel{def}{=} \mathbf{E} \times \mathbf{H} \quad (41)$$

$$\mathbf{G} \stackrel{def}{=} \mathbf{D} \times \mathbf{B} \quad (42)$$

The transformations of the state quantities and the definitions (39) ... (42) lead to the following transformations of E , \mathbf{S} and \mathbf{G} :

¹⁾ The symbol \mathbf{I} stands for the unit dyadic, and the dotless juxtaposition of two vectors (e.g. $\mathbf{E} \mathbf{D}$) stands for Gibb's dyadic product. The dot multiplication of a vector into a dyadic (tensor) (e.g. $\mathbf{v} \cdot \mathbf{E} \mathbf{D}$) gives another vector. In general $\mathbf{v} \cdot \mathfrak{T} \neq \mathfrak{T} \cdot \mathbf{v}$, i.e. \mathfrak{T} is asymmetric.

$$E' = E - \mathbf{v} \cdot \mathbf{G} - \varepsilon\mu\mathbf{v} \cdot \mathbf{S} \quad (43)$$

$$\mathbf{S}' = \mathbf{S} - \mathbf{v} E - \mathbf{v} \cdot \mathcal{G} \quad (44)$$

$$\mathbf{G}' = \mathbf{G} - \varepsilon\mu\mathbf{v} E - \varepsilon\mu \mathcal{G} \cdot \mathbf{v} \quad (45)$$

The transformations (43), (44) and (45) are perfectly general, independent of the nature of matter, in accordance with rule (III) of the introduction. The condition of linearity has been imposed to simplify the physical interpretations of the quantities defined by (39) and (40). Please note that the velocity \mathbf{v} appears as a prefactor of \mathcal{G} in (44) but as a postfactor of \mathcal{G} in (45). This means that the asymmetry in anisotropic matter is a calculational feature in the transformations of energy transport and momentum. The physical significance of (43), (44) and (45) may be more readily appreciated by the following applications.

The vectors \mathbf{S}' and \mathbf{S} give the rate at which energy is absorbed per unit area and unit time on absorbing screens having a mutual velocity \mathbf{v} . There are two contributions which account for the difference between \mathbf{S}' and \mathbf{S} ; $\mathbf{v}E$ is the extra absorption due to the translational motion of the screen and $\mathbf{v} \cdot \mathcal{G}$ represents the rate of work performed by the radiation forces (radiation pressure).

In a pure wavefield the time average of the Poynting vector \mathbf{S} can be expressed in terms of the parameters of the wavefield:

$$\mathbf{S} = E \mathbf{g}, \quad \mathbf{g} = \text{group or energy velocity} \quad (46)$$

In a moving body we expect

$$\mathbf{S}' = E' \mathbf{g}', \quad (47)$$

and \mathbf{g}' should be correlated to \mathbf{g} according to the general formula of Fizeau convection.

This can be verified indeed, if we use the wave expressions for \mathbf{G} and \mathcal{G} corresponding to (46) and (47) for \mathbf{S} . They are:

$$\mathbf{G} = \frac{E}{\omega} \mathbf{k} \quad \begin{array}{l} E = \text{energy density} \\ \mathbf{k} = \text{wave vector} \end{array} \quad (48)$$

$$\mathcal{G} = \frac{E}{\omega} \mathbf{k} \mathbf{g} \quad \begin{array}{l} \omega = \text{circular frequency} \\ \mathbf{g} = \text{group velocity} \end{array} \quad (49)$$

Using (47) together with (43) and (44), and substituting the expression (48) and (49) for \mathbf{G} and \mathcal{G} we obtain:

$$\mathbf{g}' = \frac{\mathbf{S}'}{E'} = \frac{E\mathbf{g} - E\mathbf{v} - \mathbf{v} \cdot \mathbf{k} g E/\omega}{E - \mathbf{v} \cdot \mathbf{k} E/\omega - \varepsilon\mu\mathbf{v} \cdot \mathbf{g} E} = \frac{\mathbf{g} - \mathbf{v} - \mathbf{v} \cdot \mathbf{k} g/\omega}{1 - \mathbf{v} \cdot \mathbf{k}/\omega - \varepsilon\mu\mathbf{v} \cdot \mathbf{g}}$$

This gives the first-order expression:

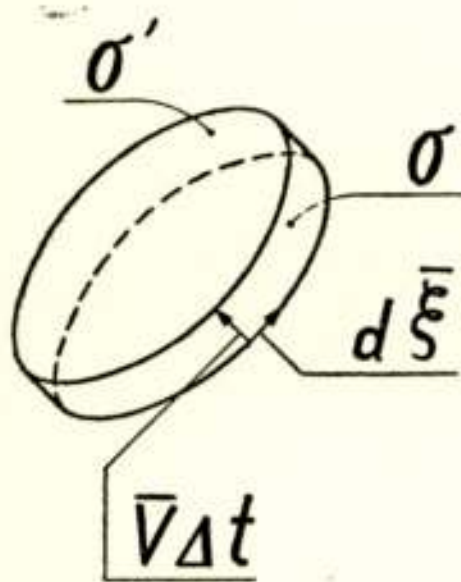
$$\mathbf{g}' = \mathbf{g} - \mathbf{v} + \varepsilon\mu\mathbf{v} \cdot \mathbf{g} \mathbf{g}, \quad (50)$$

which is identical to the first-order result obtained by means of the relativistic theorem of velocity addition for arbitrary directions of \mathbf{v} and \mathbf{g} (ref. (2) p273).

Appendix I

There are two contributions to the total time derivative of a surface integral. One is due to the intrinsic time dependence of the vector field \mathbf{A} , the other is due to the change of position of the surface with respect to the coordinate system. This leads to the definition formula:

$$\frac{d}{dt} \int \mathbf{A} \cdot d\sigma = \int \frac{\partial \mathbf{A}}{\partial t} \cdot d\sigma + \lim_{\Delta t \rightarrow 0} \frac{\int \mathbf{A} \cdot d\sigma' - \int \mathbf{A} \cdot d\sigma}{\Delta t} \quad \text{I}$$



The second term in the right hand member can be calculated using Gauss' theorem for the cylindrical volume generated by the motion of the surface (see figure 1). Keeping in mind that the vectors $d\sigma'$ and $d\sigma$ are pointing in the same direction, Gauss' law applied to the volume of figure 1 gives:

Fig. 1

Time differentiation of a surface integral

$$\Delta t \int (\text{div } \mathbf{A}) \mathbf{v} \cdot d\sigma = \int \mathbf{A} \cdot d\sigma' - \int \mathbf{A} \cdot d\sigma + \Delta t \int \mathbf{A} \cdot d\xi \times \mathbf{v} \quad \text{II}$$

The last integral can be transformed according to a well known vector rule:

$$\int \mathbf{A} \cdot d\xi \times \mathbf{v} = - \int \mathbf{A} \times \mathbf{v} \cdot d\xi = - \int \text{curl} (\mathbf{A} \times \mathbf{v}) \cdot d\sigma,$$

the transformation into a surface integral is done by means of Stokes' theorem. Substitution in II and rearrangement of terms yields:

$$\Delta t \int \{ \mathbf{v} \operatorname{div} \mathbf{A} + \operatorname{curl} \mathbf{A} \times \mathbf{v} \} \cdot d\boldsymbol{\sigma} = \int \mathbf{A} \cdot d\boldsymbol{\sigma}' - \int \mathbf{A} \cdot d\boldsymbol{\sigma}. \quad \text{III}$$

Substituting III in I gives the desired formula

$$\frac{d}{dt} \int_{\sigma} \mathbf{A} \cdot d\boldsymbol{\sigma} = \int_{\sigma} \left\{ \frac{\partial \mathbf{A}}{\partial t} + \operatorname{curl} (\mathbf{A} \times \mathbf{v}) + \mathbf{v} \operatorname{div} \mathbf{A} \right\} \cdot d\boldsymbol{\sigma} \quad \text{IV}$$

A similar formula can be derived for a volume integral $\int \rho d\tau$. Taking $\rho = \operatorname{div} \mathbf{B}$, $\int \rho d\tau = \int \mathbf{B} \cdot d\boldsymbol{\sigma}$. The formula can be applied to obtain the time derivative of this integral over a *closed* surface σ . Then we obtain:

$$\frac{d}{dt} \int \rho d\tau = \int \left\{ \frac{\partial \rho}{\partial t} + \operatorname{div} \rho \mathbf{v} \right\} d\tau \quad \text{V}$$

remembering $\operatorname{div} \operatorname{curl} = 0$.

The case of a line integral cannot be derived from formula IV in an unique way. A similar analysis, however, gives (see ref. (2) p129).

$$\frac{d}{dt} \int \mathbf{A} \cdot d\boldsymbol{\xi} = \int \left\{ \frac{\partial \mathbf{A}}{\partial t} - \mathbf{v} \times \operatorname{curl} \mathbf{A} + \operatorname{grad} \mathbf{v} \cdot \mathbf{A} \right\} \cdot d\boldsymbol{\xi} \quad \text{VI}$$

The equations IV, V and VI are special cases of a more general theorem:

Let the integral

$$\psi = \int \Phi d\varphi$$

have an invariant meaning. The field Φ is, except for an explicit time dependence, moreover subjected to a deformation, defined by the vector field $\mathbf{v} dt$, then the time derivative of ψ is

$$\frac{d\psi}{dt} = \int \left\{ \frac{\partial \Phi}{\partial t} + \underset{v}{\mathcal{L}} \Phi \right\} \cdot d\varphi$$

The symbol $\underset{v}{\mathcal{L}}$ stands for a simultaneous differential invariant of Φ and \mathbf{v} , known as the Lie derivative (see ref. 3, chapter II, § 10, and p. 111 problem II 10, 11).

Appendix II

There is a fundamental mathematical difference between the linear vector function ε relating \mathbf{E} and \mathbf{D} and the linear vector

function γ relating \mathbf{D} and \mathbf{H} . The difference is caused by a mathematical distinction between the electric and magnetic field quantities.

The simple physical devices of a pair of opposite point charges and a coil winding with current, which generate an electric and a magnetic field, respectively, emphasize already [strongly the different nature of the two kinds of fields.

The mentioned distinction is usually of no consequence unless one investigates transformation behaviour with respect to *improper* rotations (properties of mirror symmetry). The conventional notation of vector analysis does not account for this difference in behaviour. Mathematically it implies that the magnetic fields are better represented by bivector quantities. The bivector can be regarded as the vector product of two ordinary vectors. The customary procedure in vector algebra, to identify the result of this operation with an ordinary vector, is correct, only if coordinate systems are considered which are mutually related by *proper* rotations.

An inversion is a well known example of an *improper* rotation. The inversion reverses the positive directions of the coordinate axes of a system of reference. This implies that the three components of a vector change their sign, if the coordinate system is subjected to an inversion. Recalling the example of the vector-product, it will be clear that the components of a *bivector* are not affected if the system of reference is subjected to an inversion. Hence the consequences of an inversion for the equation of state of Tellegen's medium (24) are:

$$-\mathbf{D} = -\epsilon \mathbf{E} + \gamma \mathbf{H}$$

$$\mathbf{B} = -\gamma \mathbf{E} + \mu \mathbf{H}$$

Applying Neumann's principle, this equation should be identical to the original one (24) if the medium is supposed to be isotropic. The result of the identification is $\gamma = 0$, whereas ϵ and μ are allowed to have arbitrary values different from zero.

The distinction between the linear vector functions ϵ and μ on the one hand and γ on the other is known in tensor analysis as the difference between a tensor and a pseudo- or *W*-tensor. A recent text about this subject (ref. 4, p. 159) gives the information required about the possible existence of a "gyroscopic" effect (*W*-tensor) on basis of Neumann's principle for any of the 32 crystal classes.

Conclusion and Acknowledgement

A semi-classical approach dispensing with the concept of aether has been given by Professor E. G. Cullwick in his book : "Fundamentals of Electromagnetism" (5). The present paper gives an attempt to extend this point of view to the specific field of moving matter.

The author is indebted to Professor Cullwick for ample and stimulating correspondence and to Professor J. P. Schouten and Mr. L. A. W. van der Lek for many helpful and valuable discussions.

References

1. T e l l e g e n, B. D. H., Philips Res. Reports 3 (1948) p. 81.
T e l l e g e n, B. D. H., Tijdschrift Nederlands Radiogenootschap, 13 (1948) p. 73 (dutch).
 2. M a d e l u n g, E., Mathematical Tools for the Physicist, Berlin—New York, 1936.
 3. S c h o u t e n, J. A., Ricci Calculus, Berlin—London—New York, 1954.
 4. S c h o u t e n, J. A., Tensor Analysis for Physicists, Oxford, 1951.
 5. C u l l w i c k, E. G., The Fundamentals of Electromagnetism, Cambridge University press, 1949.
-

NIEUWE UITGAVEN

De redactie ontving de volgende nieuwe uitgaven:

Electronenbuizen voor batterijontvangers door E. Rodenhuis.

Van microfoon tot oor, door G. Slot.

Gegevens en schakelingen van ontvang- en versterkerbuizen, deel 3B. door N. S. Markus en J. Vink.

Vacuum Valves in Pulse Technique, door P. A. Neeteson.

In een der volgende nummers zullen deze uitgaven besproken worden.

Boekbesprekingen

Second Thoughts on Radio Theory door „Cathode Ray of Wireless World”. Uitgegeven door Iliffe and Sons, London 1955. 412 blz., 15 x 22 cm. Prijs 25 sh.

Reeds jaren lang verschijnen in *Wireless World* regelmatig artikelen, ondertekend met de schuilnaam „Cathode Ray”, waarin allerlei onderwerpen op radio-gebied op bevattelijke wijze worden besproken; het is daarbij de bedoeling van de schrijver om te laten zien dat ook in vrij elementaire onderwerpen *bij nader inzien* bijna steeds meer in zit dan men wel gedacht had. Vandaar de titel „Second Thoughts” on Radio Theory van dit onlangs verschenen boek, waarin omstreeks 40 van die artikeltjes uit *Wireless World*, wat bijgewerkt en gemoderniseerd, zijn samengevoegd. Door de heldere en vaak geestige wijze waarop de kwesties gesteld en besproken worden, zullen alle geïnteresseerden op radio-gebied — ook de meer ingewijden — met genoegen dit boek lezen.

E. O.

Radiobuizen Vademecum, door Dr. J. A. Gijsen. Uitgegeven door P. H. Brans, Antwerpen, 12de uitgave, 381 pag., 20,5 x 29 cm.

Zoals bekend is het *Buizen-Vademecum* dat geregeld door de uitgeverij Brans te Antwerpen wordt uitgegeven sedert 1952 gesplitst in drie delen. De negende uitgave die in dat jaar verscheen was uitsluitend aan zend- en ontvangbuizen gewijd. De 10de uitgave (1953) behandelde vervangingsbuizen en in 1954 werd de trilogie voltooid met de 11de uitgave, welke Televisie- en speciale buizen behandelt.

Thans ontvingen wij de 12de uitgave, een herziening van het in 1952 verschenen 1ste deel: Zend- en ontvangbuizen. Het voorwoord vermeldt dat men de gegevens van een aantal oudere buizen heeft laten vervallen. Uit het feit dat b.v. van de oude Philips A en B series nog tal van buizen zijn opgenomen moge blijken dat ook degenen die gegevens van verouderde buizen zoeken deze vaak ook in de nieuwe uitgave nog kunnen vinden.

Ongetwijfeld zullen velen zich het nieuwe werk aanschaffen gezien het aantal nieuwe zend- en ontvangbuizen dat in de laatste drie jaren aan de markt verschenen is.

H.

Uit het Nederlands Radiogenootschap

VERGADERINGEN

Sinds het verschijnen van het vorige nummer had op 17 October te Hilversum een vergadering plaats waarbij als sprekers optraden Ir K. Rodenhuis met als onderwerp: Levensduur en betrouwbaarheid van radiobuizen voor professionele toepassingen, en Dr Ir A. van Weel over het onderwerp: Fazelineariteit van televisieontvangers.

VOORGESTELDE LEDEN

G. Gaikhorst, Coosje Buskenstraat 32, Vlissingen. (PZEM, Middelburg)
 Ir L. Krul, Jan Maetsuyckerstraat 63, Den Haag. (PTT)
 C. A. Smit, Sandenburgstraat 194, Den Haag. (PTT)

NIEUWE ADRESSEN VAN LEDEN

Ir M. P. Breedveld, p/a Thierensweg 13, Naarden.
 R. Y. Drost, Rembr. v. Rijnstraat 73, Weesp.
 Ir J. A. Hammer, Koepelweg 30, Noordwijk a/Z.
 Dr Ir E. W. van Heuven, p/a N.V. Philips Gloeilampenfabrieken, Lichtgroep, Eindhoven.
 Ir J. A. Koster, Leenderweg 319, Eindhoven.
 Ir J. J. Schreuders, Hofbrouckerlaan 22, Oegstgeest.
 Ir C. J. H. A. Staal, Boerhavelaan 57, Eindhoven.
 Ir M. Steffelaar, Jonckbloetlaan 13, Eindhoven.
 Ir J. D. H. v. d. Toorn, Van Bergenlaan 4, Wassenaar.
 Ir L. R. M. Vos de Wael, Laan van Oostenburg 49, Voorburg.
 Ir A. Wieberdink, van Swietenlaan 10, Eindhoven.
 Ir M. Ziegler, c/o Philips Chilena S.A. de Productos Electricos, Casille 2687, Santiago de Chile (Chili).

OUDE NUMMERS GEVRAAGD

Een onzer leden mist van deel 10 het vierde nummer en van deel 11 het eerste nummer. Degene die deze nummers af zou kunnen staan wordt vriendelijk verzocht zich met de hoofdredacteur in verbinding te stellen.